Spin Densities and Spin Coupling in Iron–Sulfur Clusters: A New Analysis of Hyperfine Coupling Constants

J.-M. Mouesca,*,†,§ L. Noodleman,*,† D. A. Case,† and B. Lamotte‡

Department of Molecular Biology, The Scripps Research Institute, La Jolla, California 92037, and DRFMC/SESAM/SCPM, Centre d'Etudes Nucléaires de Grenoble, 17 rue des Martyrs, 38054 Grenoble Cedex 09, France

Received July 7, 1994[⊗]

We present a new analysis of ^{57}Fe isotropic hyperfine coupling constants in iron–sulfur clusters containing one, two, three, or four iron atoms. Instead of relying on a unique set of site values for ferric and ferrous ions which depend on the degree of covalency of the iron atom with the surrounding atoms and which contain a variable spin-orbit contribution, we propose the use of semi-empirical *free ion* constants $\bar{a}(Fe^{3+})$ and $\bar{a}(Fe^{2.5+})$ whose values are semiempirically found to be about −31 MHz and −32 MHz respectively (we found, in addition, −38 MHz for the pure core-polarization constant $\bar{a}_c(Fe^{2+})$, in excellent agreement with theoretical calculations). These are *transferrable* from one system to another, and can be combined with estimated covalency factors to define "site values." These values allow us to derive a set of spin projection coefficients for a variety of iron–sulfur clusters (two to four irons, and some mixed-metal complexes) in different oxidation states. These can be compared to those deduced from proposed spin-coupling schemes. For the $[Fe_4S_4]^{3+}$ cluster, which forms the active site of the high potential iron protein (HiPIP), we conclude that the best simple spin state, within a pairwise model in which two ions dimers combine to make a tetramer, is $|S_{mv},S_{ferric},S_t\rangle = |^7/_2,3,^1/_2\rangle$, and not $|^9/_2,4,^1/_2\rangle$ as is often assumed. The stabilization of this spin state is rationalized in terms of spin frustration. For 4Fe ferredoxins, we find spin projection coefficients intermediate between those of the $|^7/_2,3,^1/_2\rangle$ and $|^5/_2,2,^1/_2\rangle$ states, whereas the aconitase cluster (both with and without substrate) has coefficients intermediate between those of the states $|^9/_2,4,^1/_2\rangle$ and $|^7/_2,3,^1/_2\rangle$. In aconitase, the change upon release of substrate appears to be accompanied by a relocalization of the mixed-valence pair. We also report analyses for mixed-metal complexes of the form $[MFe_3S_4]^{n+}$, with (M,*n*) = (V,2), (Co,2), (Ni,1), (Zn,1), and (Mo,3), in an attempt to gain some insight into a wide variety of polynuclear spin-coupling schemes.

I. Introduction

The iron–sulfur proteins belong to a large family of metalloproteins that have, at their active sites, one or more metal ions: mostly iron, but also copper, manganese, molybdenum, cobalt, etc. Among the many types of active sites in iron-sulfur proteins (as well as in synthetic complexes that mimic their magnetic, electronic and redox properties[1–3]), we focus our attention here on those made of one to four iron atoms (including 3Fe heterometal complexes $[MFe_3S_4]^{n+}$, with M = Mo, V, Co, Ni, and Zn). In those systems, each iron atom is coordinated to four sulfur atoms, some being "inorganic" bridging ligands whereas others belong to side chains of cysteine amino acids, linking the cluster to the protein. The ligand field exerted on the iron atom is sufficiently weak to result in a high-spin configuration for the irons in both oxidized ($S(Fe^{3+}) = ^5/_2$) and reduced ($S(Fe^{2+}) = 2$) states.

These clusters exhibit a rich variety of electronic properties. One finds localized, trapped valence structures, as in the 2Fe ferredoxin in its reduced state (whose active site contains ferric- and ferrous-type monomers antiferromagnetically coupled to a spin S_t of $^1/_2$), and partially (or entirely) delocalized electronic structures, as in 4Fe ferredoxin and HiPIP systems (which are characterized by the presence of at least one delocalized mixed-valence pair of iron atoms with formal charge +2.5). This diversity of electronic structures, in turn, is reflected in a variety of ways of magnetically coupling the iron atoms. One probe for understanding various spin-coupling schemes is offered by ^{57}Fe isotropic hyperfine coupling constants. We show here that it is possible to correlate many of these measurements for a large number of systems with different numbers of iron atoms per cluster, redox states, and spin-coupling schemes.

A common approach to this problem defines a set of "site values" or "intrinsic" hyperfine constants a(Fe), which are later combined to yield properties of the entire cluster. For some systems, values of $a(Fe^{2+}) = -22$ MHz and $a(Fe^{3+}) = -20$ MHz seem appropriate,[4] but other values have been proposed,[5,6] for example −27 and −23 MHz. These quantities represent the hyperfine coupling expected for an isolated rubredoxin-like monomer, and are assumed to be transferrable to larger clusters. However, the site values depend on a covalency factor which may differ from one system to another. For ferrous ions, the site value also contains a spin–orbit contribution which may change from one cluster to another. Here we attempt to describe these effects in a systematic and quantitative way. As input, we will consider experimental isotropic hyperfine constants for

† The Scripps Research Institute.
‡ Centre d'Etudes Nucléaires de Grenoble.
§ Now at the DRFMC/SESAM/SCPM, Centre d'Etudes Nucléaires de Grenoble, 17 rue des Martyrs, 38054 Grenoble Cedex 09, France.
⊗ Abstract published in *Advance ACS Abstracts,* July 15, 1995.

(1) Lovenberg, W., Ed. *Iron-Sulfur Proteins*; Academic Press: New York: 1973, Vols. I and II; 1977, Vol. III.
(2) Spiro, T. G., Ed. *Iron-Sulfur Proteins*; Wiley-Interscience Publication: New York, 1982.
(3) Matsubara, H.; Katsube, Y.; Wada, K., Eds. *Iron-Sulfur Protein Research*; Japan Scientific Societies Press & Springer-Verlag: Tokyo and Berlin, 1987.
(4) Papaefthymiou, V.; Girerd, J. J.; Moura, I.; Moura, J. J. G.; Münck, E. *J. Am. Chem. Soc.* **1987**, *109*, 4703.
(5) Kent, T. A.; Huynh, B. H. *Advances in Inorganic Biochemistry*; Marzilli, L. G., Eichhorn, G. L., Eds.; Elsevier: Amsterdam, 1984; Vol. 6, pp 163–233.
(6) Werst, M. M.; Kennedy, M. C.; Houseman, A. L. P.; Beinert, H.; Hoffman, B. M. *Biochemistry* **1990**, *29*, 10533.

0020-1669/95/1334-4347$09.00/0 © 1995 American Chemical Society

Table 1. Experimental $A^{exp}(Fe_i)$ (MHz)

system	Fe^{3+}	$Fe^{2.5+}$	Fe^{2+}	$a_{test}(Fe)$	ref
desulforedoxin	−21.0		−21.3		23
rubredoxin	−22.6		−23.4		4, 24
$Fe(SPh)_4$			−22.0		23
av.	**−21.8**		**−22.2**		
Parsley Fd.	−46.4		+19.6	−26.8	17, 18
spinach Fd.	−47.4		+21.0	−26.4	17, 18
lividus Fd.	−47.9		+21.5	−26.4	19
putidaredoxin	−49.7		+23.3	−26.4	20
adrenodoxin	−49.7		+25.3	−24.4	18
av.	**−48.2**		**+22.1**	**−26.1**	
C. vinosum HiPIP ox.	+20.3 (×2)	−30.4 (×2)		−20.2	9b
$[Fe_4S_4(S\text{-}2,4,6\text{-}i\text{-}Pr_3C_6H_2)_4]^-$	+20.2 (×2)	−32.0 (×2)		−23.6	62
$[Fe_4S_4(SCH_2Ph)]^-$	+18.6 (×2)	−33.1 (×2)		−29.0	63
av.	**+19.7** (×2)	**−31.8** (×2)		**−24.2**	
$[Fe_3S_4]^0$ *D. gigas* Fd II	+15.6	−19.1 (×2)		−22.6	4
$[Fe_3S_4]^0$ *P. furiosus* Fd	+16.2	−19.8 (×2)		−23.4	42
av.	**+15.9**	**−19.4** (×2)		**−23.0**	
$[Fe_3S_4]^{1+}$ *A. vinelandii* (cubane-like)	−41, +18, +5				35
av.	**−41, +11.5** (×2)			**−18.0**	
$(EtN)_3[Fe_3S_4(SPh)_4]$ (linear)	**+13.5, −18.0** (×2)			**−22.5**	36
Av2 protein		−29.7 (×2)	+15.7 (×2)	−28.0	32
B. stearothermophilus Fd		−30.3 (×2)	+16.0 (×2)	−28.6	9a, 32
$[Fe_4S_4(S\text{-}p\text{-}C_6H_4Br)_4]^{3-}$		−31.8 (×2)	**15.1** (×2)	−32.4	33
$2[Fe_4S_4(SR)_4]^{3-}$CpFd		−28.3 (×2)	+14.4 (×2)	−27.8	64
$2[Fe_4Se_4(SR)_4]^{3-}$CpFd		−32.1 (×2)	+15.3 (×2)	−33.6	34
av.		**−30.4** (×2)	**+15.3** (×2)	**−30.2**	

Table 2. Experimental $A^{exp}(Fe_i)$ (MHz)

system	Fe^{3+}	$Fe^{2.5+}$	Fe^{2+}	$a_{test}(Fe)$	ref
Av_2/Urea (S_t=3/2)		**−7.8** (×2)	**−4.1** (×2)	**−23.8**	32
$[Fe_4S_4(SC_6H_{11})_4]^{3-}$ (S_t=3/2)		−8.9 (×2)	−8.9 (×2)	−35.6	33
$2[Fe_4Se_4(SR)_4]^{3-}$ CpFd (S_t=3/2)		−3.8 (×2)	−3.8 (×2)	−15.2	34
av.		**−6.4** (×2)	**−6.4** (×2)	**−25.4**	
$2[Fe_4Se_4(SR)_4]^{3-}$ CpFd (S_t=7/2)	**+8.1**		**−10.4** (×3)	**−23.1**	34
aconitase		b_2: −36	a: +29		6
(substrate bound)		b_3: −40	b_1: +15		
av.		**−38** (×2)	**+22** (×2)	**−32**	
Aconitase (1st choice)		b_2: −32.6	a: +38.6		6
(substrate free)		b_3: −37.0	b_1: ∼+15		
av.		**−34.8** (×2)	∼**+27** (×2)	**−16**	
Aconitase (2nd choice)		a: −38.6	b_2: +32.6		6
(substrate free)		b_3: −37.0	b_1: ∼+15		
av.		**−37.8** (×2)	∼**+24** (×2)	**−28**	
$[CoFe_3S_4]^{2+}$ in *D. gigas* Fd II	+28.7	−34.7 (×2)		−40.7	39
$[CoFe_3S_4(Smes)_4]^{2-}$	+30.6	−32.5, −34.9		−36.8	40
av.	**+29.6**	**−34.2** (×2)		**−38.7**	
$[ZnFe_3S_4]^{1+}$ in *D. gigas* Fd II		−14.0, −14.8	+6.6	−22.2	43
$[ZnFe_3S_4]^{1+}$ in *P. Furiosus* Fd		−14.3, −15.7	<7	<−23	42
av.		**−14.7** (×2)	∼**+6.6**	∼**−22.8**	
$[NiFe_3S_4(PPh_3)(SEt)_3]^{2-}$		−15.7, −21.5	+17.4	−19.8	41
$[NiFe_3S_4]^+$ in *P. furiosus* Fd		−21.8, −22.4	+17.4	−26.8	42
av.		**−20.3** (×2)	**+17.4**	**−23.3**	
$[MoFe_3S_4(SR)_4(3,6\text{-}R'_2cat)]^{3-}$	+17.6	−24.2 (×2)		−30.8	44
$(Et_4N)[MoFE_3S_4(SEt)_4(dmpe)]$	+20.0	−28.1 (×2)		−36.2	38
av.	**+18.8**	**−26.1** (×2)		**−33.4**	
$(Ph_4P)[VFe_3S_4(S\text{-}p\text{-}C_6H_4Me)_3(DMF)_3]$	**+21.8**	**−30.0** (×2)		**−38.2**	38

various systems as well as theoretical covalency factors derived from density functional theory calculations performed on models of the 1Fe, 2Fe, and 4Fe systems.

II. Basic Concepts

II-1. Covalency Factors. Let us denote by $A^{exp}(Fe_i)$ the isotropic hyperfine constant measured for the iron Fe_i. Experimental values for a wide variety of iron−sulfur clusters are collected in Tables 1 and 2. The iron atoms are in a high-spin configuration, and spin transfer occurs from the ligands to the minority spin (unfilled) metal d-orbitals. This spin transfer has the effect of reducing the observed hyperfine interactions. We define a covalency factor $d_B(Fe_i)$ as the ratio of the spin population $\Delta P(Fe_i)$ to the maximum spin population we would expect in the valence-bond limit, which is $2S(Fe_i)$ (i.e. 4 for Fe^{2+} and 5 for Fe^{3+}):

$$d_B(Fe_i) = \Delta P(Fe_i)/2S(Fe_i) \quad (1)$$

$d_B(Fe_i) = 1$ corresponds to the pure ionic, or valence-bond (VB) limit, and $\Delta P(Fe_i) \equiv |P^\alpha(Fe_i) - P^\beta(Fe_i)|$, where $P^\alpha(Fe_i)$ and $P^\beta(Fe_i)$ are the iron d-orbital α and β spin populations. We choose the d spin population rather than the total spin population since it is this spin that is primarily involved in the core-polarization mechanism which is important for isotropic hyperfine couplings. There is no unique way of partitioning the total spin density of a given system into the different atoms composing it; we have chosen the readily available Mulliken analysis as calculated from theoretical Xα calculations. Details of the calculations are given in Appendix A.

Table 3 gives quantum chemical values of the covalency factors for one-, two-, and four-iron systems. The spin populations of ferrous ions generally decrease as the number of iron atoms increases, as seen from the $d_B(Fe_i)$ values: 0.82 (1Fe reduced), 0.75 (2Fe reduced) and 0.72 (4Fe ferredoxin reduced). Overall, more iron atoms lead to more antiferromagnetic couplings and more covalency (metal−ligand delocalization).[7] The same trend is seen for the ferric ions: 0.71 (1Fe oxidized), 0.64 and 0.66 (in $[Fe_2S_2]^{2+}$ and $[Fe_2S_2]^{+}$, respectively), and 0.63 (ferric site in $[Fe_4S_4]^{3+}$). The ferrous ions thus are closer to their ionic limit but also show more variation in their covalency parameters. We can also see from Table 3 that the spin population is neither entirely localized on the iron atoms (VB picture for which we expect spin populations $\Delta P(Fe_i)$ of 4 for Fe^{2+} and 5 for Fe^{3+}) nor entirely delocalized over the whole cluster (MO picture, with a common value of $\Delta P(Fe_i)$ for all the iron atoms of a given system).

II-2. Spin Projection Coefficients. A second factor involved in the determination of $A^{exp}(Fe_i)$ is the spin coupling scheme adopted by the cluster. In polynuclear clusters, the monomers of spin $S(Fe_i)$ are magnetically coupled so as to result in a total spin S_t for the cluster. Different coupling schemes are possible, each resulting in a set of spin projection coefficients $K(Fe_i)$ defined by

$$K(Fe_i) = \langle S(Fe_i)_z\rangle/\langle S_{tz}\rangle = \langle \mathbf{S}(Fe_i)\cdot\mathbf{S}_t\rangle/S_t(S_t+1) \quad (2)$$

At the theoretical foundation of the definition of such coefficients $K(Fe_i)$ is the Wigner−Eckard theorem associated with the vector-model.[8,9] This model, within the context of our present study, states that two spin vectors $S(Fe_i)$ and $S(Fe_j)$ are vectorially coupled to give a resultant spin S_{ij} whose magnitude can be any of the integrally spaced values between $|S(Fe_i) - S(Fe_j)|$ and $S(Fe_i) + S(Fe_j)$. The quantity $K(Fe_i)$ gives the projection of the "local" spin onto the spin of the entire cluster. We assume here that the zero-field splitting of the individual ions is much smaller in magnitude than the spin coupling parameter J_{ij}; this situation is referred to as the "strong-coupling" limit[10] ($J_{ij} \gg D_i, D_j$).

A simple theorem states that

$$\sum_i K(Fe_i) = 1 \quad (3)$$

The theorem is easily derived by substituting the final expression in eq 2 for each $K(Fe_i)$ in eq 3 and regrouping terms. Thus the knowledge of some of the $K(Fe_i)$'s often allows us to calculate the others. We can then relate the measured hyperfine coupling constant $A^{exp}(Fe_i)$ to the intrinsic site value $a(Fe_i)$

$$A^{exp}(Fe_i) = K(Fe_i)a(Fe_i) \quad (4)$$

For simple clusters, like reduced two-iron ferredoxins, there is no ambiguity in the choice of the coupling scheme: there is only one way to couple a spin $^5/_2$ (spin of the monomer containing the ferric ion) with a spin 2 (spin of the ferrous monomer) to yield the experimentally observed $S_t = {}^1/_2$. We have[11] therefore $K(Fe^{3+}) = +{}^7/_3$ and $K(Fe^{2+}) = -{}^4/_3$. Larger clusters will generally have many possible spin couplings. Given $A^{exp}(Fe_i)$ for a system, we would like to *derive* the corresponding spin projection coefficients $K(Fe_i)$ through the use of eq 4. This requires however the knowledge of $a(Fe_i)$, which depends on the covalency factor $d_B(Fe_i)$ as well as on an orbital-related contribution which we discuss below.

II-3. "Ionic Limit" Intrinsic Hyperfine Constants. Our first step in analyzing the composition of the site value $a(Fe_i)$ is to decompose it into its two principal contributions. Those are the *core polarization* and the *orbital* terms:

$$a(Fe_i) = a_c(Fe_i) + a_l(Fe_i) \quad (5)$$

Both terms include covalency effects, in a manner specified now. The analysis of the first term $a_c(Fe_i)$ requires the definition of a quantity (referred to by replacing "a" with "$\bar{a}$") from which covalency effects have been removed:

$$\bar{a}_c(Fe_i) = a_c(Fe_i)/d_B(Fe_i) \quad (6)$$

The quantity $\bar{a}_c(Fe_i)$ is therefore essentially ionic in character and takes the explicit form

$$\bar{a}_c(Fe_i) = -g_e\beta_e g_n\beta_n \langle r^{-3}\rangle \kappa \quad (7)$$

where κ determines the polarization of the filled s orbitals

Table 3. Theoretical Covalency Parameters $d_B(Fe_i)$ for the Xα Potential[a]

system	Fe^{3+}	$Fe^{2.5+}$	Fe^{2+}
$[Fe(SCH_3)_4]^-$	0.71		
$[Fe(SCH_3)_4]^{2-}$			0.82
$[Fe_2S_2(SCH_3)_4]^{2-}$	0.64		
$[Fe_2S_2(SCH_3)_4]^{3-}$	0.66		0.75
$[Fe_4S_4(SCH_3)_4]^-$	(0.57)[b]	(0.59)[b]	
	0.63	0.66	
$[Fe_4S_4(SCH_3)_4]^{2-}$		0.66[c]	
$[Fe_4S_4(SCH_3)_4]^{3-}$		0.70	0.72
$[MoFe_3S_4(SH)_6]^{3-}$	(0.58)[d]	(0.65)[d]	
	0.64[e]	0.72[e]	

[a] All number are derived from LCAO−valence bond calculations unless stated otherwise. [b] Scattered−wave covalency parameters for d orbitals (not previously published). [c] Given for the sake of completeness although not used for our analysis. [d] SW parameters. The ratio [d]/[s + p + d] of the spin populations has been estimated from $[Fe_4S_4(SCH_3)_4]^-$ (0.95 for Fe^{3+} and $Fe^{2.5+}$) and applied to $[MoFe_3S_4(SH)_6]^{3-}$ for which only total spin populations on the irons [s + p + d] are published in ref 51 (see text). [e] Parameters derived using scaling factors (from SW to LCAO numbers) calculated from $[Fe_4S_4(SCH_3)_4]^-$ (0.64 = [0.63/0.57]0.58 for Fe^{3+} and 0.72 = [0.66/0.59]0.65 for $Fe^{2.5+}$).

(7) Noodleman, L.; Norman, J. G., Jr.; Osborne, J. H.; Aizman, A.; Case, D. A. *J. Am. Chem. Soc.* **1985**, *107*, 3418.
(8) Brink, D. M.; Satchler, G. R. *Angular Momentum*, 2nd ed.; Oxford University Press: London, 1968.
(9) (a) Middleton, P.; Dickson, D. P. E.; Johnson, C. E.; Rush, J. D. *Eur. J. Biochem.* **1978**, *88*, 135. (b) Middleton, P.; Dickson, D. P. E.; Johnson, C. E.; Rush, J. D. *Eur. J. Biochem.* **1980**, *104*, 289.
(10) (a) Guigliarelli, B.; Bertrand, P.; Gayda, J.-P. *J. Chem. Phys.* **1986**, *85*, 1689. (b) Guigliarelli, B.; More, C.; Bertrand, P.; Gayda, J.-P. *J. Chem. Phys.* **1986**, *85*, 2774. (c) Sage, J. T.; Xia, Y.-M.; Debrunner, P. G.; Keough, D. T.; de Jersey, J.; Zerner, B.; *J. Am. Chem. Soc.* **1989**, *111*, 7239.
(11) Gibson, J. F.; Hall, D. O.; Thornley, J. H. M.; Whatley, F. R. *Proc. Natl. Acad. Sci. U.S.A.* **1966**, *56*, 987−990.

Table 4. Core Polarization Terms for Fe^{2+} and Fe^{3+} Free Ions

ion	$\langle r^{-3}\rangle^a$ (au)	$g_e\beta_e g_n\beta_n\langle r^{-3}\rangle$ (MHz)	κ^b	$\bar{a}_c$ (MHz)
Fe^{2+}	+5.08	87.6	+0.43	−37.8
Fe^{3+}	+5.72	98.7	+0.35	−34.6

[a] From ref. 13 [b] From ref 14.

induced by net spin in the magnetic orbitals.[12] Table 4 gives theoretical estimates based on the unrestricted Hartree−Fock method for $\langle r^{-3}\rangle$[13] and for κ,[14] yielding $\bar{a}_c(Fe^{3+}) = -34.6$ MHz and $\bar{a}_c(Fe^{2+}) = -37.8$ MHz. How these values compare with values derived from the experimental data will be shown in section III.

Dealing with $a_l(Fe_i)$ requires a little more care. This is a *pseudo-contact* (second-order) term resulting from an orbital (spin−orbit) contribution and taking the following form:[15]

$$a_l(Fe_i) = 2\beta_e g_n \beta_n \langle r^{-3}\rangle \, \mathrm{Tr}(\Delta g(Fe_i))/3 \qquad (8)$$

This contribution is proportional to the trace of the $\Delta\mathbf{g}(Fe_i)$ tensor, giving the deviation of $g(Fe_i)$ (as it would be measured from experiment) from the free electron value $g_o = 2.0023$. This last contribution is expected to be small for spherically symmetric ferric ions but not for ferrous ions. Covalency effects intervene in $a_l(Fe_i)$ in two ways. At first, $\Delta\mathbf{g}(Fe_i)$ does include a covalency-corrected spin−orbit coupling constant (for a detailed discussion on the subject, see for example the review article by Owen and Thornley[16]). Second, there is a covalency factor related to the use of (occupied) molecular orbitals in the calculation of $\Delta\mathbf{g}(Fe_i)$. To derive an approximate covalency-free term (where "covalency" refers here to the second type of effect), we *define* the quantity

$$\Delta\bar{g}(Fe_i) = \Delta g(Fe_i)/d_B(Fe_i) \qquad (9)$$

$\Delta\bar{\mathbf{g}}(Fe_i)$ is not the same as a "conventional" ionic $\Delta\mathbf{g}$ tensor, but it will serve our purpose well enough, as will become clear at the end of section III. In close analogy to eq 6, $\bar{a}_l(Fe_i)$ equals $a_l(Fe_i)/d_B(Fe_i)$, and we obtain the same equation as eq 5 but with quantities marked with a bar, so that the form now taken by the experimental isotropic hyperfine constant is:

$$A^{exp}(Fe_i) = \bar{a}(Fe_i) d_B(Fe_i) K(Fe_i) \qquad (10)$$

where the product $d_B(Fe_i)K(Fe_i)$ corresponds to the effective spin population of the iron Fe_i in the coupled system. If $\bar{a}(Fe_i)$ were a constant (independent of the number of irons in the cluster), eq 10 would be like McConnell's relation in the aromatic free radicals, for which the isotropic hyperfine coupling of a proton is proportional to the spin density on the $2p_z$ orbital of the adjacent carbon.

III. 1Fe and 2Fe Systems

The fact that ferric sites involve mainly core-polarization (and little orbital) contribution is *central* to our strategy for a systematic understanding of the isotropic hyperfine coupling constants $A^{exp}(Fe_i)$. In such a case, $\bar{a}(Fe^{3+})$ $(=a(Fe^{3+})/d_B(Fe^{3+}))$ is expected to be nearly constant for all systems containing formal ferric ions. As an example, consider the 1Fe system in its oxidized state (for which $K(Fe^{3+}) = 1$) and the 2Fe system in its reduced state (for which $K(Fe^{3+}) = +^7/_3$). From $A^{exp}(Fe^{3+}) = -21.8$ MHz in the 1Fe system[4,9,10] (see also Table 1), we deduce from eq 10: $\bar{a}(Fe^{3+}) \approx -30.9$ MHz. From $A^{exp}(Fe^{3+}) = -48.2$ MHz in the 2Fe,[17−20] we obtain $\bar{a}(Fe^{3+}) \approx -31.3$ MHz. This constancy suggests that a general value for $\bar{a}(Fe^{3+})$ is −31 MHz (see Table 6). This semiempirical value is reasonably close to (but still a little smaller than) the theoretical estimate of $\bar{a}_c(Fe^{3+})$, which is −34.6 MHz (Table 4). The difference (3.6 MHz) could arise for example from overestimates in covalency factors or deficiencies in the unrestricted Hartree−Fock estimate of κ. However, if we ascribe the difference to a small orbital contribution, we could estimate the corresponding average ferric site value from a combined use of eqs 8 and 9. We would then obtain $\mathrm{Tr}(\Delta g(Fe^{3+}))/3 \approx 0.025$ for the ferric site of 1Fe and 2Fe centers. This value compares well with measurements done on Fe^{3+} in ZnS, yielding 0.02,[21] and falls within the expected range for $\mathrm{Tr}(\Delta g(Fe^{3+}))/3$: 0.01−0.04.[22] As long as this value is small, and not subject to great variations (in contrast to the case of the ferrous sites), it will be good enough to consider a common (and transferable) value of $\bar{a}(Fe^{3+}) = -31$ MHz.

We can therefore use the fact that there is little orbital contribution expected for a ferric ion (the d electron distribution is spherically symmetric) to obtain a set of site values for the different systems encountered in our study. We estimated the value of $\bar{a}(Fe^{3+})$ from the use, among other things ($A^{exp}(Fe^{3+})$ and $K(Fe^{3+})$), of the theoretical covalency factors $d_B(Fe^{3+})$. However, the theoretical quantity which is most relevant is not so much the absolute magnitude of $d_B(Fe_i)$ for a given system as the ratio of those factors for two systems. Hence, assuming nearly constant $\bar{a}(Fe^{3+})$ value, we obtain

$$a(Fe^{3+})_{2Fe} = a(Fe^{3+})_{1Fe} \frac{d_B(Fe^{3+})_{2Fe}}{d_B(Fe^{3+})_{1Fe}} \qquad (11a)$$

$$a(Fe^{3+})_{4Fe} = a(Fe^{3+})_{1Fe} \frac{d_B(Fe^{3+})_{4Fe}}{d_B(Fe^{3+})_{1Fe}} \qquad (11b)$$

The resulting site values are therefore "calibrated" to the 1Fe oxidized state[4,23,24] (taken to be −21.8 MHz, Table 1), and are listed in Table 5. We note that these site values for the 1Fe, 2Fe, and 4Fe clusters are similar: the average value is −20.5 MHz, very close to the commonly defined ferric site value of −20 MHz[4], which gives an indication about the validity of this approach for the ferric ions.

We cannot follow as simple a procedure for a ferrous ion, since the orbital contribution may differ from one system to another. This can be illustrated by comparing the 1Fe system in its reduced state with the ferrous ion of a reduced 2Fe system. For the former, with $A^{exp}(Fe^{2+}) = -22.2$ MHz (and $K(Fe^{2+}) = 1$) we deduce, from eq 10, $\bar{a}(Fe^{2+}) \approx -27.3$ MHz whereas with the latter, from $A^{exp}(Fe^{2+}) = +22.1$ MHz and $K(Fe^{2+}) = -^4/_3$,

(12) Abragam, A.; Bleaney, B. *Electron Paramagnetic Resonance of Transition Ions*; Oxford University Press: London, 1970; Chapters 17-5 and 17-6 and references therein.
(13) Freeman, A. J.; Watson, R. E. *Magnetism*; Rado, G. T., Suhl, H., Eds.; Academic Press: New York, 1965; Vol. II A, p 167.
(14) Watson, R. E.; Freeman, A. J. *Hyperfine Interactions*; *Academic Press*: New York, 1967; p 53.
(15) Reference 12, Chapter 7-6.
(16) Owen, J.; Thornley, J. H. M. *Rep. Prog. Phys.* **1966**, *29*, 675−728.
(17) Dunham, W. R.; Bearden, A. J.; Salmeen, I. T.; Palmer, G.; Sands, R. H.; Orme-Johnson, W. H.; Beinert, H. *Biochim. Biophys. Acta* **1971**, *253*, 134.
(18) Fritz, J.; Anderson, R. E.; Fee, J.; Palmer, G.; Sands, R. H.; Tsibris, J. C. M.; Gunsalus, I. C.; Orme-Johnson, W. H.; Beinert, H. *Biochim. Biophys. Acta* **1971**, *253*, 110.
(19) Anderson, R. E.; Dunham, W. R.; Sands, R. H.; Bearden, A. J.; Crespi, H. *Biochim. Biophys. Acta* **1975**, *408*, 306.
(20) Münck, E.; Debrunner, P. G.; Tsibris, J. C. M.; Gunsalus, I. C. *Biochemistry* **1972**, *11*, 855.
(21) Title, R. S.; *Phys. Rev.* **1963**, *131*, 623.
(22) Guigliarelli, B.; More, C.; Bertrand, P.; Gayda, J.-P.; *J. Chem. Phys.* **1986**, *85*, 2774−2778.
(23) Moura, I.; Huynh, B. H.; Hausinger, R. P.; LeGall, J.; Xavier, A. V.; Münck, E. *J. Biol. Chem.* **1980**, *255*, 2493−2498.
(24) Schultz, C.; Debrunner, P. G. *J. Phys. Colloq.* **1976**, *37*, 153.

Table 5. Estimated Site Values $a(Fe_i)$ (MHz)

system	$a(Fe^{3+})$	$a(Fe^{2.5+})$	$a(Fe^{2+})$
rubredoxin ox.	−21.8		
rubredoxin rd.			−22.3
$[Fe_2S_2]^+$	−20.7		−16.6
$[Fe_2S_2]^{2-}$	−19.9		
$[Fe_4S_4]^{3+}$	−19.6	−21.1	
$[Fe_3S_4]^0$: $S_t = 2$	−19.6[a]	−21.4[b]	
$[Fe_4S_4]^+$: $S_t = 1/2$		−22.5	−18.0
$[Fe_4S_4]^+$: $S_t = 3/2$ (pairw)		∼−24	∼−24
$[Fe_4S_4]^+$: $S_t = 3/2$ (deloc)			∼−25.4 for $Fe^{2.25+}$
$[Fe_4S_4]^+$: $S_t = 7/2$	$\|a(Fe^{3+})\| < \|a(Fe^{2+})\|$		$\|a(Fe^{2+})\| < 23.8$
$[Fe_3S_4]^+$: $S_t = 1/2$	3(−18.0)		
$[Fe_3S_4]^+$: $S_t = 5/2$	2(20.7[c]) −18.1[b]		
$[MoFe_3S_4]^{3+}$: $S_t = 3/2$	−19.9	−23.1	

[a] Default ferric value, taken from $[Fe_4S_4]^{3+}$. [b] Deduced using the ferric value from a different system, as indicated. [c] Ferric value, taken from $[Fe_2S_2]^+$.

we have $\bar{a}(Fe^{2+}) \approx -22.0$ MHz, which is substantially different from the preceding value. The orbital term is proportional to $\Delta g(Fe^{2+})$, which is expected to be positive, from both theory[25,26] and experiment,[23,27] for reduced rubredoxin-like systems. Therefore, $\bar{a}_l(Fe^{2+})$ should also be positive.

In order to estimate this orbital contribution, consider the case of the one-iron system. The experimental (although indirectly obtained) **g** tensor for rubredoxin (*Clostridium pasteurianum*) is (2.11, 2.19, 2.00)[27] and that of desulforedoxin (*Desulfovibrio gigas*) is (2.08, 2.02, 2.20).[23] Both tensors have a common value of $\mathrm{Tr}(\Delta\mathbf{g}(Fe^{2+}))/3 \approx 0.10$. We can therefore estimate from eqs 8 and 9 that $\bar{a}_l(Fe^{2+}) \approx +10.7$ MHz (using $d_B(Fe^{2+}) = 0.82$). Since $A^{exp}(Fe^{2+})$ is measured to be −22.2 MHz, we estimate $\bar{a}(Fe^{2+})$ to be around −27.3 MHz and consequently $\bar{a}_c(Fe^{2+})$ to be −38 MHz. This value is close to the theoretical one (−37.8 MHz in Table 4).

In both cases (Fe^{3+} and Fe^{2+}), we have seen that the (somewhat approximate) eqs 8 and 9 yield reasonable estimates for $\bar{a}_l(Fe_i)$. The parameters here derived for 1Fe systems $\bar{a}(Fe^{3+})$ (≈ -31 MHz) and $\bar{a}(Fe^{2+})$ ($=\bar{a}_c(Fe^{2+})+\bar{a}_l(Fe^{2+}) \approx -27$ MHz) are in fact equivalent to the constants $Q_1 = -30$ MHz and $Q_2 = -27$ MHz, estimated respectively for a ferric and a ferrous ion, as proposed recently by Bertrand,[28] although we emphasize that Q_2 is not expected to be transferable among clusters.

Using our values, we can estimate the orbital contribution for the ferrous site of the 2Fe reduced system. It is important to see that no assumption about the site **g** tensor of the ferric ion is required. Using $\bar{a}(Fe^{2+}) \approx -22.0$ MHz and $\bar{a}_c(Fe^{2+}) \approx -38$ MHz as suggested above, we obtain directly $\bar{a}_l(Fe^{2+}) \approx +16$ MHz (to be compared to +11 MHz in the case of the 1Fe reduced system). These values, and others obtained by similar calculations are collected in Table 6. In terms of the ferrous site **g** tensor, $\bar{a}_l(Fe^{2+}) = +16$ MHz would correspond through eqs 8 and 9 to $\mathrm{Tr}(\Delta\mathbf{g}(Fe^{2+}))/3 \approx 0.14$. Let us emphasize once more that this last value has been calculated independently of the corresponding quantity on the ferric site, which does not appear anywhere in the preceding estimation of $\Delta\mathbf{g}(Fe^{2+})$. For the sake of comparison however, the use of such a simple equation as $\Delta\mathbf{g} = (+^7/_3)\Delta\mathbf{g}(Fe^{3+}) - (^4/_3)\Delta\mathbf{g}(Fe^{2+}))$ could yield

Table 6. Estimated $\bar{a}(Fe_i)$ Values (MHz)[f]

system	$\bar{a}(Fe^{3+})$	$\bar{a}(Fe^{2.5+})$	$\bar{a}(Fe^{2+})$	$\bar{a}_l(Fe^{2+})$
rubredoxin ox.	−30.9			
rubredoxin rd.			−27.3	≈+11
$[Fe_2S_2]^+$	−31.3		−22.0	≈+16
$[Fe_4S_4]^{3+}$	−31[a]	−32.2[b]		
$[Fe_4S_4]^+$: $S_t = 1/2$		−32[c]	−25.0[b]	≈+13
$[Fe_4S_4]$: $S_t = 3/2$ (pairw)		−34.3	−34.3	≈+4
$[Fe_4S_4]$: $S_t = 3/2$ (deloc)			−35.7[d] for $Fe^{2.25+}$	≈0[e]
$[Fe_4S_4]$: $S_t = 7/2$	−31[a]		$\|\bar{a}(Fe^{2+})\| < 34$	>4
$[Fe_3S_4]^0$: $S_t = 2$	−31[a]	−32.6[b]		

[a] Default value, from average over Rub. ox. and $[Fe_2S_2]^+$. [b] Deduced by using the default value for the ferric site. [c] Using the default value from $[Fe_4S_4]^{3+}$. [d] Estimation using $d_B(Fe^{2.25+}) \sim 0.7$. [e] Estimation using $\bar{a}(Fe^{2.25+}) \approx -36$ MHz. [f] $\bar{a}(Fe^{2+}) = \bar{a}_c(Fe^{2+}) + \bar{a}_l(Fe^{2+})$ with $\bar{a}_c(Fe^{3+}) \approx -34$ MHz, $\bar{a}_c(Fe^{2+}) \approx -38$ MHz (and $\bar{a}_c(Fe^{2.5+}) \approx -36$ MHz).

an independent estimate of $\mathrm{Tr}(\Delta\mathbf{g}(Fe^{2+}))/3$ from the knowledge of $\mathrm{Tr}(\Delta\mathbf{g})/3 \approx 1.96-2.00 = -0.04$, and from $\mathrm{Tr}(\Delta\mathbf{g}(Fe^{3+}))/3 \approx 0.01-0.04$. We would obtain in this way $\mathrm{Tr}(\Delta\mathbf{g}(Fe^{2+}))/3 \approx 0.05-0.10$. An exact value of $\Delta\mathbf{g}(Fe^{2+})$ is secondary to our purpose, which is ultimately to derive sets of spin coupling coefficients, and our analysis will rely primarily on estimated values for $\bar{a}(Fe^{3+})$ (and $\bar{a}(Fe^{2.5+})$: see section V).

IV. Site Value a_{test}

We now introduce the parameter a_{test} which is based on the experimental isotropic hyperfine constants $A^{exp}(Fe_i)$. It gives new qualitative as well as semiquantitative insights. On the basis of the relation $\sum_i K(Fe_i) = \sum_i [A^{exp}(Fe_i)/a(Fe_i)] = 1$, we can define

$$a_{test} \equiv \sum_i A^{exp}(Fe_i) = \frac{\sum_i K(Fe_i) a(Fe_i)}{\sum_i K(Fe_i)} \qquad (12)$$

This is just a weighted average of the iron site values $a(Fe_i)$, the weights being the spin projection coefficients $K(Fe_i)$. If all the sites of a system had the same value $a(Fe_i)$, this common site value would be a_{test}. Tables 1 and 2 report a_{test} for the clusters we consider in this paper. There are roughly two classes, those whose values center around −21 MHz ± 15% (1Fe systems, $[Fe_4S_4(SR)_4]^-$ (except when R = CH_2Ph), $[Fe_3S_4]^{0/+}$ and heterometal 3Fe complexes containing Zn), and those whose a_{test} values are significantly larger in magnitude (2Fe systems, $[Fe_4S_4(SR)_4]^{3-}$ (including aconitase) and heterometal 3Fe complexes containing Co, Mo, and V). We suspect (from the form of eq 12) that the departure of a_{test} from −22 MHz is related to inequivalence of the site values $a(Fe_i)$. Consider a cluster made of n_i iron sites of one type (with the associated quantities $A^{exp}(Fe_i)$, $a(Fe_i)$, and $K(Fe_i)$) and n_j iron sites of a second type. For the systems considered in this paper, $n_i + n_j = 2$, 3, or 4. As an example, "i" can stand for "ferrous" and "j" for "ferric" ions in a reduced 2Fe cluster. We have therefore the following system of equations:

$$n_i K(Fe_i) + n_j K(Fe_j) = 1 \qquad (13a)$$

$$n_i A^{exp}(Fe_i) + n_j A^{exp}(Fe_j) = a_{test} \qquad (13b)$$

When $a(Fe_i) = a(Fe_j)$ ($=a_{test}$), $K(Fe_i)$ is simply $A^{exp}(Fe_i)/a_{test}$. When $a(Fe_i) \neq a(Fe_j)$ we obtain:

$$K(Fe_i) = \frac{1}{n_i}\frac{a_{test} - a(Fe_j)}{a(Fe_i) - a(Fe_j)} \qquad (14a)$$

$$K(Fe_j) = \frac{1}{n_j}\frac{a(Fe_i) - a_{test}}{a(Fe_i) - a(Fe_j)} \qquad (14b)$$

(25) (a) Stone, A. J. *Proc. R. Soc. London, A* **1964**, *271*, 424–434. (b) Atherton, N. M. *Electron Spin Resonance—Theory and Applications*; Sugden, T. M., Ed.; John Wiley & Sons Inc.: New York, 1973, *Chapter 6*. (c) Bertrand, P.; Gayda, J.-P. *Biochim. Biophys. Acta* **1979**, *579*, 107–121.
(26) Noodleman, L.; Baerends, E. J. *J. Am. Chem. Soc.* **1984**, *106*, 2316.
(27) Winkler, H.; Schultz, C.; Debrunner, P. D. *Phys. Lett.* **1979**, *69A*, 360–363.
(28) Bertrand, P. *Inorg. Chem.* **1993**, *32*, 741–745.

Since the intrinsic site values are always negative, we can deduce from the signs of the A^{exp}'s the signs of the spin projection coefficients. Consider the example of the reduced 2Fe ferredoxin systems (for which $n_i = n_j = 1$). Since $K(Fe^{3+})$ and $K(Fe^{2+})$ are of opposite sign, $a(Fe^{3+})$ and $a(Fe^{2+})$ must both be smaller than (or both be greater than) a_{test} ($a_{test} - a(Fe_j)$ and $a(Fe_i) - a_{test}$ have to be of opposite sign). Which of the two situations is correct can often be decided by the magnitude of a_{test}. We argued above that $a(Fe^{3+})$ is roughly conserved, with an average value of about -20 ± 2 MHz. The 2Fe systems exhibit larger values of a_{test} (mean of -26.1 MHz, Table 1), which implies that $|a_{test}| > |a(Fe^{3+})|$ and therefore (from the negative sign of $K(Fe^{2+})$) that $|a(Fe^{3+})| > |a(Fe^{2+})|$, using eq 14a. Since we estimated already $a(Fe^{3+}) = -20.4$ MHz and $a(Fe^{2+}) = -16.8$ MHz, we obtain nothing quantitatively new. However from the rough constancy of $a(Fe^{3+})$ (due to the absence of orbital contribution for a ferric ion), the measured value of $A^{exp}(Fe^{3+})$ is determined (almost) solely by the spin-coupling scheme. Hence, this approach will often allow us to deduce approximate spin-coupling schemes in more complex systems. The next section gives a variety of examples of this sort of analysis.

V. Three and Four Iron Systems

V-1. $[Fe_4S_4]^{3+}$ and $[Fe_3S_4]^0$. In this section, we derive sets of spin projection coefficients for different 3Fe and 4Fe systems. The basic conclusions are collected in Tables 5–8, which report estimated values for a, $\bar{a}$ and the spin projection coefficients K. As a first illustration, consider $[Fe_4S_4]^{3+}$; Figure 1a gives a flow-chart of the algorithm used to derive the quantities of interest. This cluster has a mixed-valence pair $Fe^{2.5+}$–$Fe^{2.5+}$ and a ferric pair Fe^{3+}–Fe^{3+}. We start with $\bar{a}(Fe^{3+}) = -31$ MHz, that we have deduced from the 1Fe and 2Fe systems, and with the experimental (Table 1) and theoretical (Tables 3 and 6) data which are listed under "INPUT" in Figure 1a. Under "PROCESS" are then listed sequentially the operations leading to the quantities we want to know, listed under "OUTPUT": spin projection coefficients for Fe^{3+} and $Fe^{2.5+}$ (Table 8), site values a (Table 5), and a mixed-valence intrinsic site value $\bar{a}(Fe^{2.5+}) = -32.2$ MHz (Table 6).

As a check of this last value, consider the cubane-like three-iron cluster $[Fe_3S_4]^0$, which contains formally a mixed-valence pair and a *single* ferric ion. The flow-chart of Figure 1a can again be used, with the only difference that the K-sum rule yields $K(Fe^{2.5+}) = [1 - K(Fe^{3+})]/2$ rather than $K(Fe^{2.5+}) = [1 - 2K(Fe^{3+})]/2$ as for the 4Fe cluster. Note that the theoretical covalency factors for the 4Fe cluster have been used for this reduced 3Fe cluster, resulting in $\bar{a}(Fe^{2.5+}) = -32.6$ MHz, in good agreement with that evaluated for the oxidized 4Fe cluster (-32.2 MHz).

The relative constancy of $\bar{a}(Fe^{2.5+})$ from $[Fe_4S_4]^{3+}$ to $[Fe_3S_4]^0$ (≈ -32.4 MHz on average) shows that the orbital contributions in both systems must be similar. From the theoretical values of $\bar{a}_c(Fe^{3+}) \approx -34.6$ MHz and $\bar{a}_c(Fe^{2+}) \approx -37.8$ MHz, we estimate that $\bar{a}_c(Fe^{2.5+}) \approx -36$ MHz. Consequently, for an ion of the mixed-valence pair, we would have $\bar{a}_l(Fe^{2.5+}) = \bar{a}(Fe^{2.5+}) - \bar{a}_c(Fe^{2.5+}) \approx +3$ or 4 MHz. This is much smaller than that observed for a ferrous ion ($\approx +11$ MHz and $+16$ MHz for 1Fe and 2Fe clusters respectively, as shown above). This suggests that we can, in first approximation, treat orbital terms of $Fe^{2.5+}$ sites as we did for Fe^{3+} sites, assuming therefore a transferable value of $\bar{a}(Fe^{2.5+})$, as we did for $\bar{a}(Fe^{3+})$, on the basis that $\bar{a}_c(Fe^{2.5+})$ is strictly transferable whereas $\bar{a}_l(Fe^{2.5+})$ is small.

V-2. $[Fe_4S_4]^+$ ($S = 1/2$). Consider next the case of reduced 4Fe clusters. We will use a flow-chart similar to that for the oxidized 4Fe cluster (see Figure 1b). The mixed-valence pairs of the oxidized (3+) and reduced (1+) clusters differ for our problem only in the value of $\bar{a}_l$, which should be small in both cases. Moreover, theoretical calculations show that the site $\mathbf{g}(Fe^{2.5+})$-tensors for $[Fe_4S_4(SCH_3)_4]^-$ and $[Fe_4S_4(SCH_3)_4]^{3-}$ are very similar. The necessary "INPUT" quantities are taken again from Tables 1, 3, and 6, and the results are reported in Tables 5, 6, and 8a. We find in particular that $\bar{a}(Fe^{2+}) \approx -25$ MHz and, therefore, $\bar{a}_l(Fe^{2+}) \approx +13$ MHz (using $d_B(Fe^{2+}) = 0.72$: see Table 3).

For this cluster $\bar{a}_l(Fe^{2+}) \approx +13$ MHz, which is comparable with ferrous sites in 1Fe and 2Fe systems ($+11$ and $+16$ MHz, respectively), but considerably larger than the corresponding

Table 7

(a) Calculated $K(Fe_i)$: Three-Iron Systems (Xα Potential)

system	Fe^{3+}	$Fe^{2.5+}$	Fe^{2+}	M^{n+}
$[Fe_3S_4]^+$				
$S = 1/2$	$+2.33, 2(-0.67)^a$			
$S = 1/2$	$+1.33, 2(-1.67)^b$			
semiempirical	$+2.28, 2(-0.64)$			
$[Fe_3S_4]^+$				
$S = 5/2$	$-0.71, 2(+0.86)^c$			
semiempirical	$-0.80, 2(+0.90)$			
$[Fe_3S_4]^0$				
$S = 2$	-0.83^d	$+0.92^d$		
semiempirical	-0.81	$+0.91$		
$[CoFe_3S_4]^{2+}$				
$S = 1/2$	-1.67^e	$+1.83^e$		-1.00^e
$S = 1/2$	-1.42^f	$+1.64^f$		-0.58^f
semiempirical	-1.51	$+1.62$		-0.73
$[MoFe_3S_4]^{3+}$				
$S = 3/2$	-1.00^g	$+1.10^g$		-0.20^g
$S = 3/2$	-0.85^h	$+1.10^h$		-0.35^h
semiempirical	-0.96	$+1.24$		-0.51
	-0.95^n	$+1.13^n$		-0.32^n
$[VFe_3S_4]^{2+}$				
$S = 3/2$	-0.85^i	$+1.10^i$		-0.35^i
semiempirical	-1.11	$+1.42$		-0.73
$[ZnFe_3S_4]^+$				
$S = 5/2$		$+0.79^j$	-0.57^j	0.00^j
$S = 5/2$		$+0.53^k$	-0.06^k	0.00^k
semiempirical		$+0.65$	-0.31	0.00
$[NiFe_3S_4]^+$				
$S = 3/2$		$+1.10^l$	-0.80^l	-0.40^l
$S = 3/2$		$+0.90^m$	-0.67^m	-0.13^m
semiempirical		$+0.90$	-0.81	$+0.01$

(b) Spin States for 3Fe Systems

ref	$S(Fe^{3+}–Fe^{3+})$	$S(Fe^{3+})$	S_t
a	2	5/2	1/2
b	3	5/2	1/2
c	5	5/2	5/2

ref	$S(Fe^{2.5+}–Fe^{2.5+})$	$S(Fe^{3+})$	S_t
d	9/2	5/2	2

ref	$S(Fe^{2.5+}–Fe^{2.5+})$	M^{n+}	$S(M^{n+})$	$S(Fe^{3+}–M^{n+})$	S_t
e	9/2	Co^{2+}	3/2	4	3/2
f	7/2	Co^{2+}	3/2	3	3/2
g	9/2	Mo^{3+}	1/2	3	3/2
h	9/2	Mo^{3+}	3/2	3	3/2
i	9/2	V^{2+}	3/2	3	3/2

ref	$S(Fe^{2.5+}–Fe^{2.5+})$	M^{n+}	$S(M^{n+})$	$S(Fe^{2+}–M^{n+})$	S_t
j	9/2	Zn^{2+}	0	2	5/2
k	7/2	Zn^{2+}	0	2	5/2
l	9/2	Ni^{2+}	1	3	3/2
m	7/2	Ni^{2+}	1	2	3/2

[n] Using adapted Scattered-wave calculation results from ref 51.

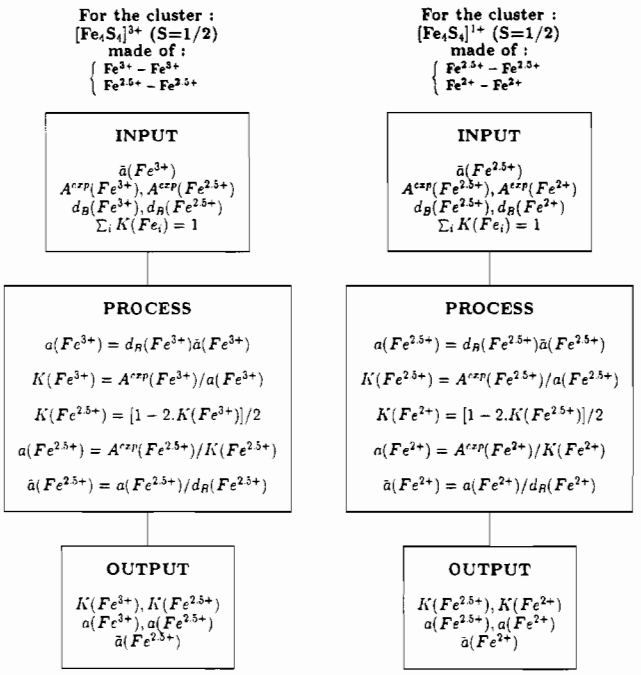

Figure 1. Flow chart of the algorithm for generating site values $a(Fe^{3+})$, $a(Fe^{2.5+})$, and $a(Fe^{2+})$, and corresponding spin projection coefficients $K(Fe_i)$ from experimental isotropic hyperfine parameters A^{exp} and covalency parameters d_B. Two cases are examined: (a) $[Fe_4S_4]^{3+}$ and (b) $[Fe_4S_4]^{+}$. Case b also uses the output from case a.

Table 8

(a) Calculated $K(Fe_i)$: Four-Iron Systems

system	Fe^{3+}	$Fe^{2.5+}$	Fe^{2+}
$[Fe_4S_4]^{3+}$			
$S = {}^1/_2$	-1.33^a	$+1.83^a$	
	-1.00^b	$+1.50^b$	
	-0.67^c	$+1.17^c$	
semiempirical	**−1.01**	**+1.51**	
$[Fe_4S_4]^{+}$			
$S = {}^1/_2$		$+1.83^d$	-1.33^d
		$+1.50^e$	-1.00^e
		$+1.17^f$	-0.67^f
semiempirical		**+1.35**	**−0.85**
$S = {}^3/_2$		$+0.39^g$	$+0.11^g$
semiempirical		**+0.33**	**+0.17**
$S = {}^7/_2$	-0.56^h		$+0.52^h$
semiempirical	**−0.41**		**+0.47**

(b) Spin States for 4Fe Systems

ref	$S(Fe^{2.5+}-Fe^{2.5+})$	$S(Fe^{3+}-Fe^{3+})$	S_t
a	$^9/_2$	4	$^1/_2$
b	$^7/_2$	3	$^1/_2$
c	$^5/_2$	2	$^1/_2$
ref	$S(Fe^{2.5+}-Fe^{2.5+})$	$S(Fe^{2+}-Fe^{2+})$	S_t
d	$^9/_2$	4	$^1/_2$
e	$^7/_2$	3	$^1/_2$
f	$^5/_2$	2	$^1/_2$
ref	$S(Fe^{2+}-Fe^{2+})$	$S(3Fe^{2+})$	S_t
g[i]	4	2	$^3/_2$
h	4	6	$^7/_2$

[i] With averaging on $Fe^{2+}-Fe^{3+}$.

orbital contribution for an ion of the mixed-valence pair. This can be rationalized by examining the orbital energy diagrams for $[Fe_4S_4]^{2+}$ and $[Fe_4S_4]^{1+}$ clusters.[7,29] In the case of a $Fe^{2.5+}$ ion, the relevant occupied molecular orbital is $20a_1$ so that the calculation of the corresponding intrinsic $\mathbf{g}(Fe^{2.5+})$ tensor, and hence of $\bar{a}_i(Fe^{2.5+})$, involves transitions from orbital $20a_1$ (and lower) to the lowest unoccupied orbital $9a_2$ (and higher). However, we can see from the energy level diagram (Figure 4 of ref 7) that the gap $20a_1-9a_2$ is large ($\sim$4000 cm^{-1}), due to the presence of resonance delocalization effects. If we consider now one of the two ferrous ions of the cluster $[Fe_4S_4]^{+}$ cluster, with occupied orbitals $20a_1$ and $9a_2$ (depicted as $OC2^{29}$), the calculation of the intrinsic $\mathbf{g}(Fe^{2+})$ tensor now involves a smaller energy gap (about 800 cm^{-1}) between $9a_2$ and the empty orbitals $14b_2$ and above and therefore results in a larger orbital contribution to the corresponding hyperfine coupling constant.

V-3. Aconitase. Now we consider the 4Fe4S reduced aconitase in its enzyme-substrate complex form.[6] The main difference with more "conventional" reduced 4Fe ferredoxins resides in the fact that one site (denoted "a", made formally of a ferrous ion) has a different local coordination. It serves as the binding site for the substrate (citrate converted to isocitrate). In the substrate-bound form (ES) the site Fe_a is coordinated to three sulfurs belonging to the 4Fe4S cluster itself, and to three oxygens (two bonds with the citrate/isocitrate and one with a water molecule). Both ENDOR and Mössbauer measurements on ^{57}Fe are available so that the signs of the hyperfine couplings, as derived from Mössbauer measurements,[30] can be readily transferred to the ENDOR results.[6] For the substrate-free system (E), there remains on the Fe_a site only a hydroxyl anion as a terminal ligand. Only ENDOR measurements are available for the hyperfine coupling parameters; the corresponding Mössbauer measurements for hyperfine parameters are not available because the requirements for sample purity are more stringent for Mössbauer spectroscopy, and only a single isomer shift value for Fe_a has been reported.[30] The lack of isomer shifts, quadrupole splittings, and hyperfine data for all sites is an indication of the experimental difficulties encountered with Mössbauer spectroscopy in the substrate-free system. Therefore, and for the sake of consistency, we will work in both cases (ES and E) with ENDOR measurements and consistently use the notation of Werst et al.[6]

In the case of (ES), the mixed-valence pair is located on the sites Fe_{b_2} and Fe_{b_3} with hyperfine couplings of −36 MHz and −40 MHz. Using a common site value of −22.5 MHz (from Table 5), we find $K(Fe_{b_2}) = +1.60$ and $K(Fe_{b_3}) = +1.78$ so that $K(Fe_{b_1}) + K(Fe_a) = -2.38$. For these latter two irons, we have $A^{exp}(Fe_{b_1}) \approx +15$ MHz and $A^{exp}(Fe_a) = +29$ MHz. Consequently, we can estimate the common ferrous site value for Fe_a and Fe_{b_1} from the ratio $[A^{exp}(Fe_a) + A^{exp}(Fe_{b_1})]/[K(Fe_{b_1}) + K(Fe_a)]$ which is a $(Fe^{2+}) = -18.5$ MHz. Hence the use for (ES) of site values analogous to those derived from "conventional" reduced 4Fe ferredoxins ($a(Fe^{2.5+}) \approx -22.5$ MHz and $a(Fe^{2+}) \approx -18.5$ MHz) seems to be appropriate; the fact that the measured hyperfine values for aconitase have a larger magnitude than that of more "conventional" reduced 4Fe ferredoxins (see Tables 1 and 2) is most probably related to the spin projection coefficients themselves. This suggests that aconitase and reduced ferredoxins have a different spin-coupling scheme; we discuss this in section VI-2. We have finally $K(Fe_{b_1}) = [A^{exp}(Fe_{b_1})/a(Fe^{2+})] = -0.81$ and $K(Fe_a) = [A^{exp}(Fe_a)/a(Fe^{2+})] = -1.57$. The two ferrous sites appear to be distinct. This is probably related to the fact that the cluster in the (ES) form is bound to the substrate at the site *a* occupied by a ferrous ion. This iron is coordinated with three oxygens (more electronegative than sulfur) whose effect is to inductively draw charge to Fe_a, and to the oxygen ligands from the rest of the cluster. This can be seen from the change in isomer shift at Fe_a from substrate-free to substrate-bound form in both the

(29) (a) Noodleman, L. *Inorg. Chem.* **1991**, *30*, 246. (b) Noodleman, L. *Inorg. Chem.* **1991**, *30*, 256.

Table 9. Calculated $K(Fe_i)$: $[Fe_4S_4]^+$ Aconitase

system	$Fe^{2.5+}$	Fe^{2+}
$S = {}^1/_2$	$+1.83^a$	-1.33^a
	$+1.50^b$	-1.00^b
substrate bound		
b_2	+1.60	
b_3	+1.78	
$a + b_1$		$2 \times (-1.19)$
substrate free		
b_2	$+1.45^c$	
b_3	$+1.64^c$	
$a + b_1$		$2 \times (-1.04)^c$
a	$+1.72^d$	
b_3	$+1.64^d$	
$b_1 + b_2$		$2 \times (-1.18)^d$

[a] State $|S(Fe^{2.5+}-Fe^{2.5+}) = {}^9/_2, S(Fe^{2+}-Fe^{2+}) = 4, S_t = {}^1/_2\rangle$. [b] State $|S(Fe^{2.5+}-Fe^{2.5+}) = {}^7/_2, S(Fe^{2+}-Fe^{2+}) = 3, S_t = {}^1/_2\rangle$. [c] Assignment originally proposed in ref 6. [d] As proposed in this work.

$[Fe_4S_4]^{2+}$ (from 0.45 to 0.85−0.89 mm/s) and the $[Fe_4S_4]^+$ (from 0.65 to 1.00 mm/s) oxidation states.[30] Werst et al.[6] proposed the following spin projection coefficients: $K(Fe_{b_2}) = +1.6$, $K(Fe_{b_3}) = +1.7$, $K(Fe_{b_1}) = -0.6$, and $K(Fe_a) = -1.1$ (compared to our values of +1.6, +1.8, −0.8, and −1.6). These differences (especially for the ferrous pair $Fe_a-Fe_{b_1}$) arises from their choice of the site values $a(Fe^{3+}) = -23$ MHz and $a(Fe^{2+}) = -27$ MHz. Their proposed ferrous site value has a large magnitude resulting in $\sum_i K(Fe_i) = +1.6$ rather than 1. Our spin projection coefficients are reported in Table 9.

Next we consider the substrate-free form of aconitase. We proceed at first with the original assignment.[6] Note that the site Fe_a is now ligated to a hydroxyl anion which exerts, at a typical Fe−O distance of 1.9−2.0 Å, a ligand-field comparable to that of a thiolate group.[31] Therefore we expect that this complex will behave in a manner similar to more "conventional" reduced 4Fe ferredoxins. Using −32.6 and −37.0 MHz, respectively, for the sites Fe_{b_2} and Fe_{b_3} assigned to the mixed-valence pair, we obtain (again using intrinsic site values from Table 5) $K(Fe_{b_2}) = +1.45$ and $K(Fe_{b_3}) = +1.64$, so that $K(Fe_{b_1}) + K(Fe_a) = -2.09$. Then, from $A^{exp}(Fe_{b_1}) \approx +15$ MHz and $A^{exp}(Fe_a) = +38.6$ MHz, we can estimate an average common ferrous site value for Fe_a and Fe_{b_1} from the ratio $[A^{exp}(Fe_a) + A^{exp}(Fe_{b_1})]/[K(Fe_{b_1}) + K(Fe_a)]$ which is $a(Fe^{2+}) = -25.6$ MHz. This value is larger than −18.5 MHz for the ES form of aconitase and other reduced 4Fe ferredoxins, and is directly related to the high value of $A^{exp}(Fe_a)$ (+38.6 MHz in the E form compared to +29 MHz in the ES form). Such a large magnitude for an average $a(Fe^{2+})$ would have to be related to a corresponding small (that is almost totally quenched) orbital contribution for these ferrous ions ($\bar{a}_c(Fe^{2+}) \approx -38$ MHz), since some covalency effect, around 0.7 for example, is already largely sufficient to produce a ferrous site value $a(Fe^{2+}) \approx -38 \times 0.7 \approx -27$ MHz. However, the **g** tensor for the substrate free form of aconitase[30] is rhombic with $g_{av} = 1.95$ and principal values (2.06, 1.93, 1.86), which are similar to those in reduced 4Fe ferredoxins. The existence of two principal values below 2.0 should be associated with a substantial orbital contribution from the ferrous pair, as in the ferredoxins. But this would contradict the notion that the ferrous contribution to $a_1(Fe^{2+})$ is quenched in substrate-free aconitase. Is there any other possible explanation?

We consider a different assignment (second choice), by identifying the mixed-valence pair with the two sites having the two greatest hyperfine coupling in magnitude, sites Fe_a and Fe_{b_3}. This is fully consistent with ENDOR data, which are ambiguous with respect to the signs of the couplings. Moreover, this behavior seems characteristic of all reduced $S = {}^1/_2$ $[Fe_4S_4]^+$ clusters, and is also consistent with current theoretical models, both pairwise[9] and nonlinear.[29] We emphasize the following critical point: this hypothesis is testable when more accurate and complete Mössbauer data are obtained, including, in particular, magnetic hyperfine data, so that both the signs and magnitudes of the hyperfine fields can be determined. This suggestion of ours implies that the transition from substrate-bound to substrate-free is accompanied by a change of localization of the mixed-valence pair. This new assignment is also suggested by the consideration of a_{test} which is found between −27 and −32 MHz for the substrate-bound form (ES), as well as for more conventional 4Fe reduced ferredoxins where $S_t = {}^1/_2$. For the substrate-free complex, the first choice proposed above yields $a_{test} \approx -16$ MHz. Such a low value results immediately in $|a(Fe^{2.5+})| < |a(Fe^{2+})|$ (using eq 14), but this result is strange and unexpected. The second assignment that we propose yields $a_{test} \approx -28$ MHz. We would then have $A^{exp}(Fe_a) = -38.6$ MHz and $A^{exp}(Fe_{b_3}) = -37.0$ MHz resulting (again using $a(Fe^{2.5+}) = -22.5$ MHz from Table 5) in $K(Fe_a) = +1.72$, $K(Fe_{b_3}) = +1.64$ and $K(Fe_{b_1}) + K(Fe_{b_2}) = -2.36$. As in the case of ES, we can estimate a common ferrous site value from the ratio $[A^{exp}(Fe_{b_1}) + A^{exp}(Fe_{b_2})]/[K(Fe_{b_1}) + K(Fe_{b_2})]$, $a(Fe^{2+}) \approx -20.1$ MHz. This value is now more reasonable. There is still an inequivalence between the sites Fe_{b_1} and Fe_{b_2} to be explained. This will be treated in section VI-2, once we have introduced a spin-coupling model for aconitase.

A reviewer has commented that the relatively high value of the isomer shift of reduced substrate-free aconitase for the labile Fe_a, which he reports (unpublished data) as 0.59 mm/s, is larger, by about 0.05 mm/s, than for two other sites, and questions whether this is consistent with Fe_a forming one site of a mixed-valence pair. There are two relevant points here. First, there are clearly experimental difficulties in obtaining good and complete data for analysis in this system, and parameter values can change when complete data sets, including magnetic hyperfine data, are analyzed. In fact, 0.05 mm/s is a fairly small difference for isomer shifts compared with typical experimental uncertainties. For example, the reported isomer shift value for Fe_a is 0.65 mm/s in the literature.[30] Second, since the cysteine thiolate and hydroxyl ligand fields on their respective iron sites should differ, even a delocalized $Fe_a-Fe_{b_3}$ pair will not be precisely equivalent, and one should expect some asymmetry in charge and spin distribution, giving "intermediate" rather than "complete" delocalization. These issues are discussed in ref 29 under the category of "effects of localizing forces". There is also the possibility of temperature dependent electron hopping between sites of the delocalized mixed-valence pair and the ferrous pair. Since magnetic hyperfine spectra, whether by ENDOR or Mössbauer spectroscopy, are collected at very low temperatures, while isomer shifts and quadrupole splittings are often determined from higher temperature data, the temperature dependence of the Mössbauer data and parameters should be carefully investigated.

V-4. $[Fe_4S_4]^+$ ($S > {}^1/_2$). Next we consider $[Fe_4X_4]^+$ (X = S, Se) systems having $S_t = {}^3/_2$. These can have both pairwise[32] as well as entirely delocalized[33,34] states. The Av2 protein in urea has measured hyperfine couplings of $A^{exp}(Fe^{2.5+}) = -7.8$

(30) Beinert, H.; Kennedy, M. C. *Eur. J. Biochem.* **1989**, *186*, 5.
(31) Huheey, J. E. *Inorganic Chemistry—Principles of Structure and Reactivity*, 2nd ed., Harper International: 1978.
(32) Lindahl, P. A.; Day, E. P.; Kent, T. A.; Orme-Johnson, W. H.; Münck, E. *J. Biol. Chem.* **1985**, *260*, 11160.
(33) Carney, M. J.; Papaefthymiou, G. C.; Spartalian, K.; Frankel, R. B.; Holm, R. H. *J. Am. Chem. Soc.* **1988**, *110*, 6084.
(34) Auric, P.; Gaillard, J.; Meyer, J.; Moulis, J.-M. *Biochem. J.* **1987**, *242*, 525−530.

MHz and $A^{exp}(Fe^{2+}) = -4.1$ MHz, and hence $a_{test} = -23.8$ MHz. The experimental hyperfine constants are all negative, and therefore, the four coupling coefficients must be positive. We have two possibilities for the relative magnitudes of $a(Fe^{2+})$ and $a(Fe^{2.5+})$:

$$|a(Fe^{2+})| < |a_{test}| = 23.8 < |a(Fe^{2.5+})| \quad (15a)$$

$$|a(Fe^{2+})| > |a_{test}| = 23.8 > |a(Fe^{2.5+})| \quad (15b)$$

Using the mixed-valence site values from 4Fe ferredoxins ($a(Fe^{2.5+}) = -22.5$ MHz) yields $K(Fe^{2.5+}) \approx +0.35$, $K(Fe^{2+}) \approx +0.15$, and $a(Fe^{2+}) = -27.9$ MHz, which fits with eq 15b. However, in systems where the extra electron appears to be almost totally delocalized over the entire cluster, one expects more nearly equal site values for $Fe^{2.5+}$ and Fe^{2+}. Using a_{test} as a common site value yields $K(Fe^{2.5+}) \approx +0.33$ and $K(Fe^{2+}) \approx +0.17$. The values of the spin projection coefficients themselves are not changed significantly but we note that the use of qualitative information from eqs 14 and 15 helps to define a range of appropriate site values. Other $S_t = {}^3/_2$ systems yield only one hyperfine parameter for the four iron sites. For such spin-delocalized $S_t = {}^3/_2$ systems, we have a common (but averaged) hyperfine constant of $A^{exp}(Fe^{2.25+}) = -6.4$ MHz, resulting in a site value of −25.4 MHz (which is of course the value of a_{test} for that system). This is close to a_{test} obtained for the Av2/urea $S_t = {}^3/_2$ system, so that the four iron sites appear to have equivalent intrinsic site values around −24 or −25 MHz, irrespective of whether the spin density is localized by pairs or delocalized over the whole cluster. This, in return, suggests that there is, in these systems, little orbital contribution to the ferrous sites (as noted above, with no orbital contribution, the ferrous site value is expected to be around −27 MHz).

The selenium-substituted $[Fe_4Se_4]^+$ clusters in *Clostridium* ferredoxin having $S_t = {}^7/_2$ are formally composed of one ferric ion, antiferromagnetically coupled to each of the three remaining ferrous ions, resulting in a unique ferric site with $A^{exp}(Fe^{3+}) = +8.1$ MHz and three equivalent $A^{exp}(Fe^{2+}) = -10.4$ MHz. First, let us consider what constraints we can get from eq 14 and the fact that a_{test} is −23.1 MHz. From $K(Fe^{2+}) > 0$, $K(Fe^{3+}) < 0$ and evidence from other clusters that $|a(Fe^{3+})| < 23.1$, we find $|a(Fe^{3+})| < |a(Fe^{2+})| < |a_{test}|$. From Table 3, we expect therefore a rather small covalency factor for Fe^{3+} ($d_b = 0.63$), and a site value of about −19.5 MHz. This would imply that $K(Fe^{3+}) = 0.41$ and $K(Fe^{2+}) = +0.47$. We note that $K(Fe^{3+})$ is sensitive and $K(Fe^{2+})$ is insensitive to the assumed value of $a(Fe^{3+})$.

For 4Fe reduced ferredoxin systems with total spin $S_t = {}^1/_2$, we have well defined mixed-valence and ferrous pairs, leading to a 2−2 pattern of hyperfine interactions. For large total spin however, the two ions of the mixed-valence pair should become more distinguishable, changing from $Fe^{2.5+}$−$Fe^{2.5+}$ when $S_t = {}^1/_2$ to Fe^{2+}−Fe^{3+} when $S_t = {}^7/_2$. This reflects a transition from a 2−2 pattern (a delocalized mixed-valence pair and a ferrous pair) to a 3−1 pattern (a localized mixed-valence pair and a ferrous pair or, equivalently, three ferrous and one ferric ion[29]). Consequently, this could affect the amount of orbital contribution present on the ferrous ions, since we have two "true" ferrous ions for $S_t = {}^1/_2$ and three for $S_t = {}^7/_2$. We have already seen from analysis of the experimental data that the orbital contribution to the ferrous site value is (partially) quenched when $S_t = {}^3/_2$ (with a corresponding large $a(Fe^{2+})$). This empirical trend continues for $S_t = {}^7/_2$, since the observed a_{test} values for $S_t = {}^1/_2$, ${}^3/_2$, and ${}^7/_2$ give a steadily decreasing trend of −30, −25, and −23 MHz, respectively.

V-5. $[Fe_3S_4]^+$. There are two known structures for $[Fe_3S_4]^+$ clusters: a cubane type, structurally related to the oxidized form[35] of the cluster $[Fe_3S_4]^0$ considered above, and a linear one.[36] For the cubane-like structure, the total spin S_t is ${}^1/_2$ and the three observed isotropic hyperfine coupling constants are: $A^{exp}(Fe_1) = -41 \pm 3$ MHz, $A^{exp}(Fe_2) = +18 \pm 3$ MHz and $A^{exp}(Fe_3) = |5 \pm 3|$ MHz.[35] Kent *et al.* proposed a positive sign for $A^{exp}(Fe_3)$, but the task of determining it seemed difficult (see footnote on p 6575 of ref 35). The use of a_{test} can help here. If $A^{exp}(Fe_3) > 0$, a_{test} would be $\approx \sim -18$ MHz whereas, if $A^{exp}(Fe_3) < 0$, a_{test} would be ≈ -28 MHz. The cubane is made formally of three ferric sites so that a common site value of −18 to −19 MHz would be quite reasonable while −28 MHz is much too large. It was later found[37] that the use of a single site value of −18 MHz in the model[35] of Kent *et al.* gave a better fit to the data. Since, from its definition, a_{test} represents the best choice of a common site value for such a system, we propose $A^{exp}(Fe_3) > 0$ and, as a consequence, $K(Fe_i) = A^{exp}(Fe_i)/a_{test}$, that is $K(Fe_1) = +2.28$, $K(Fe_2) = -1.00$ and $K(Fe_3) = -0.28$.

For the linear structure, the coupling of the central ferric ion was measured to be $A^{exp}(Fe_2) = +13.5$ MHz whereas the two others were found to be equivalent with a hyperfine coupling of $A^{exp}(Fe_1) = A^{exp}(Fe_3) = -18.0$ MHz. For the latter, we can use a ferric site value determined by using the covalency factor of a ferric ion in the oxidized 2Fe system: + 0.64, resulting in $a(Fe^{3+}) = -20$ MHz. We have $K(Fe_1) = K(Fe_3) = +0.90$ and, from the K sum rule, $K(Fe_2) = -0.80$. This last coupling coefficient results in a ferric site value (ferric in the middle of four inorganic sulfurs) of −16.9 MHz, equivalent to a covalency factor on that site of +0.55 (−16.9/−31). This low number (compared to +0.64) is not surprising since this central ion is antiferromagnetically coupled to the two others, and therefore may have partial cancellation of the spin density.

V-6. $[MFe_3S_4]^{n+}$: M = V, Co, Ni, Zn, and Mo. We finally consider a class of mixed-metal complexes of the type $[MFe_3S_4]^{n+}$ where M stands for vanadium,[38] cobalt,[39,40] nickel,[41,42] zinc,[42,43] or molybdenum.[38,44] The electron-transport protein ferredoxin II from *D. gigas* contains a 3Fe4S cluster. This cluster can react with Fe^{2+} to give the known 4Fe4S cluster.[45] However, it has been demonstrated that other ions can also be incorporated into the vacant site of the 3Fe4S cluster such as Zn^{2+} [41] and Co^{2+}.[39] In the case of nickel, a reductive rearrangement of the linear $[Fe_3S_4(SEt)_4]^{3-}$ in the presence of $Ni(PPh_3)_3$ also yields a heterometal cubane-type cluster.[41,42] Similar results have been obtained by using the linear $[Fe_3S_4(Smes)_4]^{3-}$ (Smes = mesitylthiolate(1−))[40]. The amount of metal−ligand covalency in

(35) (a) Kent, T. A.; Huynh, B. H.; Münck, E. *Proc. Natl. Acad. Sci. U.S.A.* **1980**, *77*, 6574−6576. (b) Hu, Z.; Jollie, D.; Burgess, B. K.; Stephens, P. J.; Münck, E. *Biochemistry* **1994**, *33*, 14475−14485.
(36) Girerd, J.-J.; Papaefthymiou, G. C.; Watson, A. D., Gamp, E.; Hagen, K. S.; Edelstein, N.; Frankel, R. B.; Holm, R. H. *J. Am. Chem. Soc.* **1984**, *106*, 5941−5947.
(37) Surerus, K. K.; Kennedy, M. C.; Beinert, H.; Münck, E. *Proc. Natl. Acad. Sci. U.S.A.* **1989**, *86*, 9846−9850.
(38) Carney, M. J.; Kovacs, J. A.; Zhang, Y.-P.; Papaefthymiou, G. C.; Spartalian, K.; Frankel, R. B.; Holm, R. H. *Inorg. Chem.* **1987**, *26*, 719.
(39) Moura, I.; Moura, J. J. G.; Münck, E.; Papaefthymiou, V.; LeGall, J. *J. Am. Chem. Soc.* **1986**, *108*, 349−351.
(40) Zhou, J.; Scott, M. J.; Hu, Z.; Peng, G.; Münck, E.; Holm, R. H. *J. Am. Chem. Soc.* **1992**, *114*, 10843−10854.
(41) Ciurli, S.; Shi-bao, Y.; Holm, R. H.; Srivastava, K. K. P.; Münck, E. *J. Am. Chem. Soc.* **1990**, *112*, 8169−8171.
(42) Srivastava, K. K. P.; Surerus, K. K.; Conover, R. C.; Johnson, M. K.; Park, J.-B.; Adams, M. W. W.; Münck, E.; *Inorg. Chem.* **1993**, *32*, 927.
(43) Surerus, K. K.; Münck, E.; Moura, I.; Moura, J. J. G.; LeGall, J. *J. Am. Chem. Soc.* **1987**, *109*, 3805−3807.
(44) Mascharak, P. K.; Papaefthymiou, G. C.; Armstrong, W. H.; Foner, S.; Frankel, R. B.; Holm, R. H. *Inorg. Chem.* **1983**, *22*, 2851.
(45) Moura, J. J. G.; Moura, I.; Kent, T. A.; Lipscomb, J. D.; Huynh, B. H.; LeGall, J.; Xavier, A. V.; Münck, E. *J. Biol. Chem.* **1982**, *257*, 6259−6267.

these mixed-metal systems is not known. We will therefore first use "standard" site values from 4 Fe oxidized systems (−19.6 and −21.1 MHz respectively for $a(Fe^{3+})$ and $a(Fe^{2.5+})$) for the Co, Mo, and V complexes that contain one mixed-valence pair and a ferric ion, and "standard" site values from 4 Fe reduced systems (−22.1 and −17.5 MHz, respectively, for $a(Fe^{2.5+})$ and $a(Fe^{2+})$) for the zinc and nickel complexes that contain one mixed-valence pair and one ferrous ion. Moreover, it should be noted that some of the experimental data were difficult to analyze properly, and this is reflected in uncertainties in the hyperfine parameters of the ferrous site in the Zn complex of *Pyrococcus furiosus*.[42] The spin Hamiltonian used in ref 42 may be inadequate for analysis of this low symmetry ferrous site.

We consider first the complexes containing Co, V, and Mo. These systems all include a mixed-valence pair and a ferric ion. The addition of the heterometal results in a dramatic increase of a_{test}: −38.7, −38.2, and −33.4 MHz, respectively, compared to −23 MHz on average for $[Fe_3S_4]^0$ systems. A large negative value (−43.9 MHz) would also be found for oxidized HiPIP if a_{test} were calculated by removing one ferric contribution. We can estimate first the spin projection coefficients for the ferric and the mixed-valence ions by $K(Fe^{3+}) = [A^{exp}(Fe^{3+})/a(Fe^{3+})]$ and $K(Fe^{2.5)} = [A^{exp}(Fe^{2.5+})/a(Fe^{2.5+})]$, using the site values derived for the oxidized 4Fe clusters (see Table 5). The spin projection of the heterometal is then deduced from the K sum rule: $K(M^{n+}) = 1 - 2K(Fe^{2.5+}) - K(Fe^{3+})$, in close analogy to the procedure described in Figure 1 for $[Fe_4S_4]^{3+}$ and $[Fe_4S_4]^{1}$ clusters. These spin projection coefficients are listed in Table 7. In all three cases (Co^{2+}, Mo^{3+}, and V^{2+}), $K(M^{n+})$ is negative. From the relation

$$2[A^{exp}(Fe^{2.5+})/a(Fe^{2.5+})] + [A^{exp}(Fe^{3+})/a(Fe^{3+})] = [1 - K(M^{n+})] \quad (16)$$

and since $a(Fe^{2.5+})$ and $a(Fe^{3+})$ are nearly equal (−21.1 and −19.6, respectively), we find that a_{test} and $[1 - K(M^{n+})]$ are roughly proportional, the ratio being about −22 MHz. This value is in good agreement with the value of $a_{test} \approx -23$ MHz found above for $[Fe_3S_4]^0$ clusters (where $K(M^{n+})$ is necessarily zero). Hence, the same spin coupling techniques appear to apply to these mixed-metal clusters as to the cubane-like three-iron clusters. This is expected as long as the introduction of the heterometal does not induce significant changes in the covalency parameters of the three irons. In the case of Mo^{3+}, our attempts to estimate this change in covalency are given in Appendix B. The derived value of $K(Mo^{3+})$ varies from −0.3 to −0.5 depending on the model used (see Appendix B and Table 7). Both values are relatively small and negative, with the smaller value obtained from our rescaled covalency parameters and a values for the Mo complex (see Tables 3 and 5 and Appendix B) and the larger from the "standard" covalency and a site values of the oxidized 4Fe systems. The Fe and Mo spin projection (K) values derived from the rescaled covalency parameters also agree better with theoretical spin coupling models.

The situation is somewhat different in the case of the zinc complex since Zn^{2+} is diamagnetic (with configuration d^{10}). We therefore expect that $K(Zn^{2+}) \approx 0$ (in absence of spin transfer). The (postulated) cluster $[ZnFe_3S_4]^+$ has a total spin S_t of $^5/_2$ and contains formally a mixed-valence pair of irons and a ferrous ion. The average measured hyperfine coupling for an ion of the mixed-valence pair is $A^{exp}(Fe^{2.5+}) = -14.7$ MHz. We will use the site values of the reduced ferredoxins ($a(Fe^{2.5+}) = -22.5$ MHz). We have then directly $K(Fe^{2.5+}) \approx +0.65$. As noted previously, $A^{exp}(Fe^{2+})$ is quite uncertain. Using the value of +6.6 MHz, and setting $K(Zn^{2+})$ to zero would result in $K(Fe^{2+}) \approx -0.31$ and an estimated ferrous site value of −21.5 MHz. We note however that $K(Fe^{2+})$ is small and responds sensitively to small changes in $a(Fe^{2.5+})$, so that its exact value is also uncertain.

The spin of Ni^{2+} is 1 and that of the cluster $[NiFe_3S_4]^+$ is $^3/_2$. It formally contains a mixed-valence pair and a ferrous ion. From an average value of −20.3 MHz for $A^{exp}(Fe^{2.5+})$, we have $K(Fe^{2.5+}) \approx +0.90$, and therefore $K(Fe^{2+}) + K(Ni^{2+}) \approx -0.80$. With $A^{exp}(Fe^{2+}) = +17.4$ MHz and a site value $a(Fe^{2+})$ of about −21.5 MHz (from the Zn complex), we deduce $K(Fe^{2+}) \approx -0.81$ and $K(Ni^{2+}) \approx +0.01$. We obtain a very small value for $K(Ni^{2+})$; essentially $K(Ni^{2+}) \approx 0$. We note however that if we use a site value $a(Fe^{2+})$ as in 4Fe ferredoxins (−18.0 MHz, rather than −21.5 MHz from the Zn complex), $K(Ni^{2+})$ would have been about +0.17 while we expect $K(Ni^{2+}) < 0$ from spin coupling models (Table 7). This suggests that a ferrous ion embedded in a heterometal complex has a site value greater in magnitude than that of a ferrous ion in the 4Fe reduced ferredoxins with $S_t = {}^1/_2$.

VI. Comparison with Theoretical Spin-Coupling Models

There are a few different theoretical frameworks available to derive spin projection coefficients. The simplest conceptual scheme, which has been applied to $[Fe_4S_4]^+$ and $[Fe_4S_4]^{3+}$, was originally developed by Middleton.[9] This is a *pairwise* model, in which the spins are first coupled within two dimers; these two sub-spins of the dimers are then coupled to yield the total spin S_t. This procedure reflects the experimental observation that the ^{57}Fe isotropic hyperfine coupling constants appear in a 2−2 pattern when $S_t = {}^1/_2$. However the $[Fe_4Se_4]^+$ cluster of selenium-substituted Cp Fd reduced presents experimental evidence for the coexistence of $S_t = {}^1/_2$, $^3/_2$, and $^7/_2$ states. In the last case, a 3−1 pattern is observed for the isotropic ^{57}Fe hyperfine couplings. This leads to the development of a "nonlinear model", which allows the spin projection coefficients $K(Fe_i)$ to vary as a function of spin Hamiltonian parameters J (exchange coupling constant) and B (resonance delocalization parameter).[29] This has the effect of decreasing the magnitude of the spin projection coefficients, compared to the pairwise scheme. Here we compare the predictions of various theoretical models to the semiempirical values determined above.

VI-1. $[Fe_4S_4]^{3+}$ and $[Fe_3S_4]^0$. Consider first the pairwise model for the HiPIP oxidized cluster: $[Fe_4S_4]^{3+}$. We write $|S_{mv},S_{ferric},S_t\rangle$ for the cluster spin state, where S_{mv}, S_{ferric}, and S_t stand respectively for the spin of the mixed-valence pair, the spin of the ferric pair, and the total spin of the cluster. The most straightforward state $|^9/_2,5,^1/_2\rangle$, with maximal spins for the two dimers, does not even give the correct sign for the projection coefficients: $K(Fe^{2.5+}) = -1.50$ and $K(Fe^{3+}) = +2.00$, whereas we obtained +1.51 and −1.01 respectively (semiempirical). This problem has been recognized for some time;[46] a simple model to explain this behavior recognizes that the antiferromagnetic coupling between the two ferric ions is likely to be greater than that between other pairs of ions, so that the "spin frustration" encountered by this pair will be sufficiently large to make other states (such as $|^9/_2,4,^1/_2\rangle$, which has $K(Fe^{2.5+}) = +1.83$ and $K(Fe^{3+}) = -1.33$) become the ground state. These K's now have the correct sign but are still too large. The next possible spin state is $|^7/_2,3,^1/_2\rangle$, with $K(Fe^{2.5+}) = +1.50$ and $K(Fe^{3+}) = -1.00$, in good agreement with the semiempirical values. This conclusion has been independently deduced from an analysis of EPR and proton ENDOR studies on a synthetic analogue.[47] The next possible

(46) Noodleman, L. *Inorg. Chem.* **1988**, *27*, 3677.
(47) Mouesca, J.-M.; Rius, G.; Lamotte, B. *J. Am. Chem. Soc.* **1993**, *115*, 4714.

state is $|^5/_2,2,^1/_2\rangle$ (with $K(Fe^{2.5+}) = +1.17$ and $K(Fe^{3+}) = -0.67$), a state whose projection coefficients are definitely out of range.

It is of interest to compare this to the 3Fe reduced cluster $[Fe_3S_4]^0$. This has been modeled[48,49] as a mixed-valence pair (with spin $^9/_2$), coupled antiferromagnetically to a ferric ion (of spin $^5/_2$) resulting in a total spin S_t of 2. This model gives projection coefficients $K(Fe^{2.5+}) = +0.92$ and $K(Fe^{3+}) = -0.83$, in excellent agreement with the semi-empirical values of +0.91 and −0.81. The presence of *one* ferric ion coupled to the mixed-valence pair (in $[Fe_3S_4]^0$) results in a spin $^9/_2$ for the mixed-valence pair whereas the presence of a ferric *pair* (as for the HiPIP cluster) results in a spin $^7/_2$. This is the outcome of a competition between mechanisms favoring ferromagnetism (double-exchange) and antiferromagnetism (Heisenberg exchange) and arises naturally from models that include both effects and which contain larger Heisenberg couplings for the ferric pair than for other iron−iron pairs.[46]

VI-2. $[Fe_4S_4]^+$ and Aconitase. Consider now the case of $[Fe_4S_4]^+$ with $S_t = ^1/_2$. Our semiempirical analysis gave $K(Fe^{2.5+}) = +1.35$ and $K(Fe^{2+}) = -0.85$ (average over all the different systems considered). These spin projection coefficients are intermediate between those for $|^7/_2,3,^1/_2\rangle$ (with $K(Fe^{2.5+}) = +1.50$ and $K(Fe^{2+}) = -1.00$) and those for $|^5/_2,2,^1/_2\rangle$ (with $K(Fe^{2.5+}) = +1.17$, $K(Fe^{2+}) = -0.67$) (Table 8). It is interesting to compare the case of aconitase with that of the more "classic" reduced ferredoxin-type clusters. We will consider only average spin projection coefficients for ES and E (Table 9). For aconitase ES we have $K(Fe^{2.5+}) \approx +1.69$ and $K(Fe^{2+}) \approx -1.19$. These are intermediate between those expected for the $|^9/_2,4,^1/_2\rangle$ and $|^7/_2,3,^1/_2\rangle$ states. In the case of the substrate-free complex, with a mixed-valence pair relocalized on the sites Fe_a and Fe_{b_3}, we derived almost exactly the same coefficients (+1.68 and −1.18 respectively). These are larger in magnitude than those we obtained for the other 4Fe ferredoxins above. Since the substrate-free form is expected to be electronically similar to the standard 4Fe ferredoxins, this difference in spin states is most likely related to the change in coordination at the Fe_a site and therefore to site distortions in the aconitase complex. A distorted pseudo-cubane could easily favor a site inequivalence (Table 2) for the ferrous pair, in contrast to what is observed in other 4Fe ferredoxins. The remaining change of the measured values between ES and E appears to be due to the relocalization of the mixed-valence pair.

VI-3. $[Fe_3S_4]^+$. Considering now the cluster $[Fe_3S_4]^+$ in its cubane form, two spin states are possible.[35] Let us denote S_{23} as the spin obtained by coupling $S(Fe_2)$ and $S(Fe_3)$. There are two ways to obtain a total spin $S_t = ^1/_2$ by antiferromagnetically coupling S_{23} and $S(Fe_1)$: $S_{23} = 2$ or 3. These states are denoted $|S_{23} = 2, S_t = ^1/_2\rangle$ and $|S_{23} = 3, S_t = ^1/_2\rangle$, respectively. The first state yields $K(Fe_2) = K(Fe_3) = -0.67$, and $K(Fe_1) = +2.33$ whereas the second state yields $K(Fe_2) = K(Fe_3) = +1.33$, and $K(Fe_1) = -1.67$. We obtained by our semiempirical procedure $(K(Fe_2) + K(Fe_3))/2 = -0.64$ and $K(Fe_1) = +2.28$ in excellent agreement with the theoretical spin projection coefficients of the state $|S_{23} = 2, S_t = ^1/_2\rangle$. The experimentally determined difference between $K(Fe_2)$ and $K(Fe_3)$ discussed in paragraph V-5 can then be traced back[35] to a small admixture (1%) of the state $|S_{23} = 3, S_t = ^1/_2\rangle$ into the state $|S_{23} = 2, S_t = ^1/_2\rangle$.

Magnetic Mössbauer measurements have also been made on a similar cluster from the inactive form of beef heart aconitase[37], giving $A^{exp}(Fe_1) = -30.6$ MHz, $A^{exp}(Fe_2) = +28.1$ MHz, and $A^{exp}(Fe_3) = -10.5$ MHz. This implies that $a_{test} = -13$ MHz, which is significantly smaller than that for the $[Fe_3S_4]^+$ cubane in *A. vinelandii*, where $a_{test} = -18$ MHz (see section V-5). (More recent measurements of Hu et al. give $a_{test} = -22$ MHz[35] in *A. vinelandii*, which will not affect this conclusion.) It has been shown that the hyperfine tensor of the third iron, yielding the reported averaged value of $A^{exp}(Fe_3) = -10.5$ MHz, is very anisotropic: (−2.3,−21.9,−7.4).[37] Moreover, the application of the same model as in ref 35 (with a mixing parameter of 14% this time) yielded for $A(Fe_1)$, $A(Fe_2)$, and $A(Fe_3)$ −31.9, +28.6, and −14.7 MHz, respectively[37] (using again −18 MHz as a common site value, implicitly setting $a_{test} = -18$ MHz). This model predicts therefore for the third tensor an average value of −14.7 MHz, somewhat higher than the measured value of −10.5 MHz. This descrepancy explains in part the lower value a_{test} calculated here.

A reviewer has pointed out that the hyperfine tensors measured in these oxidized 3Fe systems present very large anisotropies, whose origin is presently unknown. However, our analysis is based on the *isotropic* components of these tensors. The separation between isotropic and anisotropic parts does not restrict the *physical* mechanisms involved for either (or both) of these. It is true that, for more "usual" systems (1Fe, 2Fe and 4Fe for example), the isotropic part dominates by far the hyperfine coupling, contrary to what is happening here. Whether the *physical* sources of this anisotropy, for these ferric ions, also have isotropic effects is not known. Our analysis for these oxidized 3Fe systems would certainly be altered if the orbital effect (or some mechanism other than the core polarization) had a large isotropic contribution, since we could no longer transfer the supposed constant $\bar{a}_c(Fe^{3+})$. This same reviewer drew to our attention recent data gained on the 3Fe cluster of *C. vinosum* hydrogenase.[50] From the data, $a_{test} = -30.7$ MHz, although the uncertainty for site 3 allows $a_{test} = -28$ MHz. However, the 3Fe cluster seems to be interacting with some paramagnetic center, allowing "for the possibility that some as yet unidentified additional Fe site may be involved in the coupling" (p 4983 of ref 50). In the absence of further information about that peculiar 3Fe system, we note only that the value of a_{test} is rather unusual: the presence of a nearby single Fe site, were it confirmed by further investigations, could well have an effect on the hyperfine couplings of this 3Fe (+1Fe?) system, and therefore on a_{test}. More information is needed on the experimental side before reaching any conclusions.

The cluster $[Fe_3S_4]^+$ in its linear form is somewhat simpler: the two outer ferric ions are coupled to a spin of 5 in a first step, and this spin is then coupled antiferromagnetically to the middle third ferric ion to give a total spin S_t of $^5/_2$. The projection coefficients are −0.71 for the middle site and +0.86 for the outer sites, in good agreement with our semi-empirical values of −0.80 and +0.90 respectively (see Table 7). We note that a small variation in the value of the spin projection coefficients of the two outer iron ions results, from the *K*-sum rule, in a larger variation in the spin projection coefficient of the (unique) central ion.

VI-4. $[MFe_3S_4]^{n+}$. For the heterometal complexes, theoretical spin coupling models are more difficult to apply, and our results are more tentative. We consider two families of clusters $[MFe_3S_4]^{n+}$ depending on whether the third iron ion is ferric (M = Mo, Co, V) or ferrous (M = Zn, Ni).

Considering first the cluster $[MoFe_3S_4]^{3+}$, we write its spin state as $|S_{mv},S(Fe^{3+}\text{-}Mo^{3+}),S_t\rangle$ where again S_{mv} stands for the spin of the mixed-valence pair, $S(Fe^{3+}-Mo^{3+})$ for the spin of

(48) Münck, E.; Papaefthymiou, V.; Surerus, K. K.; Girerd, J.-J.; *Metals in Proteins*; ACS Symposium Series; American Chemical Society: Washington, DC, 1988.
(49) Münck, E.; Kent, T. A. *Hypfine Interact.* **1986**, *27*, 161−172.
(50) Surerus, K. K.; Chen, M.; van der Zwaan, J. W.; Rusnak, F. M.; Kolk, M.; Duin, E. C.; Albracht, S. P. J.; Münck, E.; *Biochemistry* **1994**, *33*, 4980−4993.

the iron−molybdenum ion pair (with here a low spin $^1/_2$ for Mo^{3+} as suggested by theoretical calculations for a $[MoFe_3S_4(SH)_6]^{3-}$ ion[51]) and S_t for the total spin of the cluster ($S_t = {}^3/_2$). In addition to the state $|{}^9/_2,3,{}^3/_2\rangle$ ($S(Mo^{3+}) = {}^1/_2$), we have also considered the possible state $|{}^9/_2,3,{}^3/_2\rangle$, with $S(Mo^{3+}) = {}^3/_2$ (high spin). Both states have $S_{mv} > S$ (Fe^{3+}−Mo^{3+}) and are therefore compatible with the experimental signs of the hyperfine parameters ($A^{exp}(Fe^{2.5+}) < 0$ and $A^{exp}(Fe^{3+}) > 0$: see Table 2). The theoretical spin projection coefficients for the two states are listed in Table 7. Both states yield theoretical spin projection coefficients in good agreement with those derived with the alternative set of site values (from rescaled scattered-wave calculation results). We could not decide, on the basis of this study, which of the two possibilities for the spin of Mo^{3+} (low or high spin) would be the correct one.

The case of vanadium yields semiempirical spin projection coefficients of even a greater magnitude than those derived for the molybdenum compound. V^{2+} is treated as a high-spin ion ($S(V^{2+}) = {}^3/_2$) and the coefficients are identical to those of the Mo cluster (Mo^{3+} high spin). The agreement between the semiempirical and theoretical spin projection coefficients is only fair: for both Fe^{3+} and $Fe^{2.5+}$, the semiempirical estimates exceed those from the spin coupling model by 30%. We reach here a limit of our method since, at the level of the spin coupling itself, there is no difference between the heterometal clusters with molybdenum and vanadium. Both clusters still differ by their geometries as well as by different covalency effects, which could explain why the experimental measurements are distinct in the two cases. Nevertheless, the mixed-valence pair has, as in the case of the molybdenum compound, to be coupled to its maximum spin whereas the spin of Fe^{3+}−V^{2+} is lowered from 4 (maximum value) to 3.

In the case of the Co complex, we derived semiempirically $K(Fe^{2.5+}) = +1.62$, $K(Fe^{3+}) = -1.51$, and $K(Co^{2+}) = -0.73$. The cobalt ion is high-spin ($S(Co^{2+}) = {}^3/_2$). With a total cluster spin of $S_t = {}^1/_2$, $S(Fe^{3+}$−$Co^{2+})$ could be 3 or 4. Consequently we have considered the states $|{}^9/_2,4,{}^1/_2\rangle$ and $|{}^7/_2,3,{}^1/_2\rangle$. We can see however from Table 6 that the semiempirical coefficients are really intermediate between those of the two states $|{}^9/_2,4,{}^1/_2\rangle$ and $|{}^7/_2,3,{}^1/_2\rangle$ and are in better agreement with those of the latter.

The cases of the Zn and Ni complexes are very similar in many respects: both are composed of a mixed-valence pair and a ferrous ion and have comparable a_{test} values and little (or no) spin density found on the heterometal. The formal site spins are $S(Zn^{2+}) = 0$ and $S(Ni^{2+}) = 1$. For Zn, we considered the states $|{}^9/_2,2,{}^5/_2\rangle$ and $|{}^7/_2,2,{}^5/_2\rangle$, the first being expected to represent the ground state.[52] The spin projection coefficients we derive semiempirically are exactly intermediate between those deduced from these two possible spin states. For the Ni compound, we considered the states $|{}^9/_2,3,{}^3/_2\rangle$ and $|{}^7/_2,2,{}^3/_2\rangle$. Both states match the iron sites about equally.

In the case of both zinc and nickel complexes, no (or almost no) spin density is found on the heterometal. It is therefore interesting to notice that the formal cluster $[Fe_3S_4]^-$ is likely to favor the state $|{}^9/_2,2,{}^5/_2\rangle$, in which no situation of spin frustration is expected. If we consider that "classic" 4Fe reduced ferredoxins have spin projection coefficients intermediary between those of the states $|{}^7/_2,3,{}^1/_2\rangle$ and $|{}^5/_2,2,{}^1/_2\rangle$, the whole is strongly reminiscent of what we observed for HiPIP oxidized 4Fe clusters (and corresponding synthetic analogues) when compared to $[Fe_3S_4]^0$ type clusters. To the former corresponded $S_{mv} = {}^7/_2$ whereas, for the latter, we found $S_{mv} = {}^9/_2$. We have the same phenomena here, apart from some nonlinearity effects, for both $[Fe_4S_4]^+$ ($S_t = {}^1/_2$) (with S_{mv} being between $^7/_2$ and $^5/_2$) and the formal $[Fe_3S_4]^-$ (with S_{mv} between $^9/_2$ and $^7/_2$).

VII. Conclusion

Our primary aim has been to correlate and explain the experimental ^{57}Fe isotropic hyperfine coupling constants of iron atoms in different iron-sulfur systems. We have considered for that purpose systems made of one, two, three, and four iron atoms, including clusters in different oxidation states and described by different possible spin states. From density functional calculations, we have estimated the magnitude of the covalency factors for ferric, ferrous and mixed-valence ions. We then deduced $\bar{a}(Fe_i)$ constants, free from the effects of covalency, and having the following values:

$$\bar{a}(Fe^{3+}) \approx -31 \text{ MHz}$$

$$\bar{a}(Fe^{2.5+}) \approx -32 \text{ MHz}$$

Additionally, we obtained independently $\bar{a}_c(Fe^{2+}) \approx -38$ MHz. A direct estimation of $\bar{a}(Fe^{3+})$ was possible, considering the one-iron oxidized system and the oxidized site of the two-iron reduced systems. We have used this for other systems, exploiting the fact that the sum of the projection coefficients for a given system is 1. In that way we obtained estimates of $\bar{a}(Fe^{2.5+})$ and $\bar{a}(Fe^{2+})$. The orbital contribution was estimated from experimental g-tensor for reduced rubredoxin, giving $\bar{a}_l(Fe^{2+}) \approx +11$ MHz, resulting in $\bar{a}_c(Fe^{2+}) \approx -38$ MHz.

A second outcome of this study is an algorithm for obtaining spin projection coefficients. We transfer the "intrinsic" values $\bar{a}(Fe^{3+})$ and $\bar{a}(Fe^{2.5+})$ from one system to another, instead of site values $a(Fe_i)$, which are system-dependent. The quantity $\bar{a}(Fe_i)$ is determined successively for Fe^{3+} and $Fe^{2.5+}$ sites (and for Fe^{2+}, with variable values) in order of decreasing relative invariance. The K-sum rule yields $\bar{a}(Fe^{2.5+})$ from that of Fe^{3+} and $\bar{a}(Fe^{2+})$ from that of $Fe^{2.5+}$. In the case of an ion of a delocalized mixed-valence pair, the orbital contribution is, for that type of ion, sufficiently small an effect to allow us to carry on a constant value from one system to another, of the order of $\bar{a}(Fe^{2.5+}) = -32$ MHz. For reasonable estimates of covalency factors, this would correspond to a site value of $a(Fe^{2.5+})$ about −21 MHz. The ferrous ion is the most sensitive to its environment in its magnetic properties, having different orbital contribution for different systems. The site value is about −22 MHz for the reduced rubredoxin and about −17 MHz for the ferrous site of the reduced 2 iron ferredoxin as well as for the ferrous ions of the 4Fe reduced ferredoxins of total spin $^1/_2$. All these sites values are estimated from calculated projection coefficients as defined in the text.

These semiempirical projection coefficients in most cases compare well with those determined by explicitly working out the coupling scheme. For HiPIP clusters in the oxidized state the best simple description appears to be $|{}^7/_2,3,{}^1/_2\rangle$ rather than $|{}^9/_2,4,{}^1/_2\rangle$. The case of the $[Fe_4S_4]^+$ clusters is more complex, with a contrast between "standard" reduced 4Fe ferredoxins (having their four cysteine ligands), for which the spin projection coefficients are found to be intermediate between $|{}^7/_2,3,{}^1/_2\rangle$ and $|{}^5/_2,2,{}^1/_2\rangle$, and aconitase (where oxygen ligands are present on one iron atom), which has larger spin projection coefficients, found between those of the states $|{}^9/_2,4,{}^1/_2\rangle$ and $|{}^7/_2,3,{}^1/_2\rangle$. Moreover we propose that, during the transition from substrate-bound to substrate-free forms, the mixed-valence site switches from the pair b_2−b_3 to the pair a−b_3.

Similar phenomena (different localization of the mixed-valence pair in the same compound as a result of environmental

(51) Cook, M.; Karplus, M. *J. Chem. Phys.* **1985**, *83*, 6344−6366.
(52) Noodleman, L.; Case, D. A.; Sontum, S. F. *J. Chim. Phys.* **1989**, *86*, 743.

changes) has recently been observed in a related synthetic compound,[53] and it has been proposed that the mixed-valence and ferric pairs in some HiPIP proteins can switch sites dynamically on the NMR time scale at room temperature.[54]

We have shown how a semiempirical approach, combining a density functional treatment of metal−ligand covalency with experimental isotropic hyperfine coupling constants, leads to insights into patterns of spin coupling in a wide variety of polynuclear iron−sulfur complexes, including those with heterometal atoms. The semiempirical spin projection coefficients can be tested against those of various proposed spin coupling schemes. The intrinsic site hyperfine values $a(Fe_i)$ for ferrous sites are highly variable and can contain a substantial orbital term, which is connected to the presence of low-lying orbital excited states. An empirical parameter a_{test}, equal to the sum of the observed isotropic hyperfine constants $A^{exp}(Fe_i)$, can be used to check the consistency of measurements, can help to resolve ambiguities in the signs of $A^{exp}(Fe_i)$, and, in favorable cases, can provide insights into assignments of site valences and the spin-coupling pattern adopted by a cluster. We have also recently applied this methodology to obtain insights into spin coupling in the oxidized P-clusters of nitrogenase proteins.[55]

Acknowledgment. This work was supported by NIH Grant GM39915 and by a NATO travel grant, CRG-910204.

Appendix A: Experimental/Computational Section

The calculations were performed using the density functional LCAO computer program of Baerends and co-workers.[56] We chose the following models: $[Fe(SCH_3)_4]^{-/2-}$ with an exact tetrahedral arrangement of the sulfurs around the iron atom and differing from the oxidized to the reduced in that the Fe−S bond was set to 2.31 Å in the former and 2.36 Å in the latter (the overall geometry chosen in both cases was C_{2v} and the electronic structure also has C_{2v} symmetry). $[Fe_2S_2(SCH_3)_4]^{2-/3-}$ for which the geometry of the $[Fe_2S_2]$ core follows in both oxidation cases the choice made in ref 26 (the only difference introduced is in the ligands (SCH_3 instead of SH): the nuclear structure is respectively D_{2h} and C_{2v} whereas the electronic structure was in both cases C_{2v}); $[Fe_4S_4(SCH_3)_4]^{-/2-/3-}$, where the geometries of that compound in the different oxidation states are reported in refs 7 and 57 (the 1− and 2− forms have the same geometries).

The basis sets used in the calculations included triple ζ expansions of 3d and 4s orbitals for Fe (frozen core: 3s and 3p), 3s and 3p for S (frozen core: 2s and 2p), 2s and 2p for C (frozen core: 1s), and 1s for H. Polarization orbitals were added: 4p for Fe, 3d for S and C, and 2p for H. The details of the broken symmetry approach have been given elsewhere.[58] The exchange-correlation potential chosen is Xα throughout. We have verified however that the main results and conclusions of this paper were not strongly dependent on that choice by performing the same analysis based on covalency factors derived from the use of another potential (Vosko−Wilk−Nusair LSD[59] with Stoll correlation[60] and Becke exchange correction[61] added). The tables corresponding to Tables 3, 5, 6, 7, and 8 set up with this alternative potential are available as supplementary material.

Appendix B: Covalency Estimates for Mo−Fe Clusters

Here we outline the way in which we obtained an estimate of the covalency in the molybdenum cluster $[MoFe_3S_4]^{3+}$, for which there exists an Xα scattered-wave calculation[51] of the electronic structure of the model $[MoFe_3S_4(SH)_6]^{3-}$. For the spin-polarized broken-symmetry (C_s) model of that complex, two irons (formal $Fe^{2.5+}$) have positive and identical spin populations +3.06, whereas the third iron (formal Fe^{3+}) and the molybdenum (formal Mo^{3+}) have negative spin populations of, respectively, −3.07 and −0.39. These numbers represent however total spin populations (s, p, and d type) whereas our covalency parameters in Table 3 contain only d-type contributions. We therefore considered first, from SW−Xα calculations of the model $[Fe_4S_4(SCH_3)_4]^-$, the ratios of d to total (s + p + d) spin population for $Fe^{2.5+}$ (0.950) and Fe^{3+} (0.945). We applied these ratios for the corresponding iron ions in $[MoFe_3S_4(SH)_6]^{3+}$ to obtain estimates of the d-only spin populations. We then proceeded further by converting these SW-type numbers to LCAO-type numbers by using appropriate scaling coefficients as determined for $[Fe_4S_4(SCH_3)_4]^-$. All the relevant numbers are listed in Table 3. The main change between the 4Fe and Mo3Fe complexes occurs at the mixed-valence pair, with a substantial increase of ionic character upon replacing one iron by one molybdenum (from 0.66 to 0.72). The "new" site values for the Mo complex are then calculated from eqs 5 and 6, with $\bar{a}(Fe^{3+}) = -31$ MHz and $\bar{a}(Fe^{2.5+}) = -32.2$ MHz, yielding $a(Fe^{3+}) = -19.9$ MHz and $a(Fe^{2.5+}) = -23.1$ MHz. These site values are listed in Table 5.

Supporting Information Available: Tables of calculated covalency parameters and hyperfine site values and spin projection coefficients using the VSB rather than the Xα potential (8 pages). Ordering information is given on any current masthead page.

IC940784F

(53) Gloux, J.; Gloux, P.; Lamotte, B.; Mouesca, J.-M.; Rius, G. *J. Am. Chem. Soc.* **1994**, *116*, 1953−1961.
(54) Banci, L.; Bertini, I.; Ferretti, S.; Luchinat, C.; Piccioli, M. *J. Mol. Struct.* **1993**, *292*, 207−220.
(55) Mouesca, J.-M.; Noodleman, L.; Case, D. A. *Inorg. Chem.* **1994**, *33*, 4819−4830.
(56) (a) Baerends, E. J.; Ellis, D. E.; Ros, P. *Chem. Phys.* **1973**, *2*, 41. (b) Baerends, E. J.; Ros, P. *Chem. Phys.* **1973**, *2*, 52. (c) Baerends, E. J.; Ros, P. *Chem. Phys.* **1975**, *8*, 412. (d) Bickelhaupt, F. M.; Baerends, E. J.; Ravenek, W. *Inorg. Chem.* **1990**, *29*, 350. (e) Ravenek, W. In *Scientific Computing on Supercomputers*; Devreese, J. T., Van Camp, P. E., Eds.; Plenum: New York, 1989; pp 201−218. (f) Ziegler, T. *Chem. Rev.* **1991**, *91*, 651.
(57) Aizman, A.; Case, D. A. *J. Am. Chem. Soc.* **1982**, *104*, 3269.
(58) (a) Noodleman, L.; Norman, J. G. *J. Chem. Phys.* **1979**, *70*, 4903. (b) Noodleman, L. *J. Chem. Phys.* **1981**, *74*, 5737. (c) Noodleman, L.; Davidson, E. R. *Chem. Phys.* **1986**, *109*, 131. (d) Noodleman, L.; Case, D. A. *Adv. Inorg. Chem.* **1992**, *38*, 423. (e) Ziegler, T.; Rauk, A.; Baerends, E. J. *Theor. Chim. Acta* **1977**, *43*, 261. (f) Lowdin, P. O. *Rev. Mod. Phys.* **1962**, *34*, 520. (h) Lowdin, P. O. *Phys. Rev.* **1955**, *97*, 1509. (i) Benard, M. *J. Chem. Phys.* **1979**, *71*, 2546. (j) Benard, M.; Paldus, J. *J. Chem. Phys.* **1980**, *72*, 6546. (k) Fukutome, H. *Prog. Theor. Phys.* **1972**, *47*, 1156.
(59) (a) Vosko, S. H.; Wilk, L.; Nusair, M. *Can. J. Phys.* **1980**, *58*, 1200. (b) Painter, G. S. *Phys. Rev.*, **B 1981**, *24*, 4264. (c) Ceperly, D. M.; Alder, H. *Phys. Rev. Lett.* **1980**, *45*, 566.
(60) (a) Stoll, H.; Pavlidou, C. M. E.; Preuss, H. *Theor. Chim. Acta* **1978**, *149*, 143. (b) Stoll, H.; Golka, E.; Preuss, H. *Theor. Chim. Acta* **1980**, *55*, 29.
(61) (a) Becke, A. D. *J. Chem. Phys.* **1986**, *84*, 4524. (b) Becke, A. D. In *The Challenge of d and f electrons*; Salahub, D. R., Zerner, N. C., Eds.; ACS Symposium Series 394; American Chemical Society: Washington, DC, 1989; p 165.
(62) Papaefthymiou, V.; Millar, M. M.; Münck, E. *Inorg. Chem.* **1986**, *25*, 3010.
(63) Rius, G.; Lamotte, B. *J. Am. Chem. Soc.* **1989**, *111*, 2464.
(64) Thomson, C. L.; Johnson, C. E.; Dickson, D. P. E.; Cammack, R.; Hall, D. O.; Weser, U.; Rao, K. K. *Biochem. J.* **1974**, *139*, 97−103.